Appendix for Online Publication

A Equilibrium

We first outline the equilibrium conditions pertaining to the model described in section 2 and the first-order approximation studied throughout the paper.

A.1 Equilibrium conditions

The optimality conditions for the U.S. representative household are:

$$c_{Ht} = \left(\frac{1}{1+\zeta^*} + \frac{\zeta^*}{1+\zeta^*}\varsigma\right)(p_{Ht})^{-\sigma} c_t, \tag{2}$$

$$c_{Ft} = \left(\frac{\zeta^*}{1+\zeta^*}(1-\varsigma)\right)(p_{Ft})^{-\sigma} c_t, \tag{3}$$

$$1 = \mathbb{E}_t \beta_t \left(\frac{c_{t+1}}{c_t}\right)^{-1/\psi} (1+r_t). \tag{4}$$

The household's resource constraint is implied by Walras' Law so we omit it here.

The optimality conditions for the Foreign representative household are:

$$c^*_{Ht} = \left(\frac{1}{1+\zeta^*}(1-\varsigma)\right)(p^*_{Ht})^{-\sigma} c^*_t, \tag{5}$$

$$c^*_{Ft} = \left(\frac{\zeta^*}{1+\zeta^*} + \frac{1}{1+\zeta^*}\varsigma\right)(p^*_{Ft})^{-\sigma} c^*_t, \tag{6}$$

$$1 = \mathbb{E}_t \beta^*_t \left(\frac{c^*_{t+1}}{c^*_t}\right)^{-1/\psi} (1+r^*_t). \tag{7}$$

Its resource constraint, using as well Foreign firms' aggregate profits, the symmetry across varieties, and goods market clearing, is

$$c^*_t + \frac{1}{1+r^*_t} b^*_t = \frac{1}{\zeta^*} q_t p_{Ft} c_{Ft} + p^*_{Ft} c^*_{Ft} + b^*_{t-1}. \tag{8}$$

Arbitrageurs' optimality conditions are:

$$\mathbb{E}_t \frac{q_t}{q_{t+1}}(1+r^*_t) - (1+r_t) = \gamma_t \left(q_t^{-1} \frac{1}{1+r^*_t} b^{a*}_t\right) Var_t \frac{q_t}{q_{t+1}}(1+r^*_t), \tag{9}$$

$$0 = \frac{1}{1+r_t} b_t^a + q_t^{-1} \frac{1}{1+r_t^*} b_t^{a*}. \tag{10}$$

Firms' optimal pricing conditions imply:

$$p_{Ht} = \frac{\theta}{\theta - 1} p_t, \tag{11}$$

$$q_t^{-1} p_{Ht}^* = \frac{\theta_t^*}{\theta_t^* - 1} p_t, \tag{12}$$

$$q_t p_{Ft} = \frac{\theta_t}{\theta_t - 1} p_t^*, \tag{13}$$

$$p_{Ft}^* = \frac{\theta}{\theta - 1} p_t^*. \tag{14}$$

Since prices faced by households in each country have been expressed relative to the overall consumption bundles, the aggregate price indices imply:

$$1 = \left(\left(\frac{1}{1+\zeta^*} + \frac{\zeta^*}{1+\zeta^*} \varsigma \right) (p_{Ht})^{1-\sigma} + \frac{\zeta^*}{1+\zeta^*} (1-\varsigma)(p_{Ft})^{1-\sigma} \right)^{\frac{1}{1-\sigma}}, \tag{15}$$

$$1 = \left(\frac{1}{1+\zeta^*} (1-\varsigma)(p_{Ht}^*)^{1-\sigma} + \left(\frac{\zeta^*}{1+\zeta^*} + \frac{1}{1+\zeta^*} \varsigma \right) (p_{Ft}^*)^{1-\sigma} \right)^{\frac{1}{1-\sigma}}. \tag{16}$$

Combining the intermediate and final goods market clearing conditions yields

$$c_{Ht} + \zeta^* c_{Ht}^* = z_t, \tag{17}$$

$$c_{Ft} + \zeta^* c_{Ft}^* = \zeta^* z_t^*. \tag{18}$$

Finally, bond market clearing requires

$$b_t + b_t^a = 0, \tag{19}$$

$$b_t^{a*} + \zeta^* b_t^* = 0. \tag{20}$$

By Walras' Law, we have that the U.S. household's resource constraint

$$c_t + \frac{1}{1+r_t} b_t = p_t z_t + \left[(p_{Ht} - p_t) c_{Ht} + (q_t^{-1} p_{Ht}^* - p_t) \zeta^* c_{Ht}^* \right] + \left[b_{t-1}^a + q_t^{-1} b_{t-1}^{a*} \right] + b_{t-1}$$

is satisfied as well.

Equations (2)-(20) define a dynamical system of 19 equations in 19 unknowns

$$\{c_t, c_{Ht}, c_{Ft}, b_t, c_t^*, c_{Ht}^*, c_{Ft}^*, b_t^*, b_t^a, b_t^{a*}, p_t, p_{Ht}, p_{Ft}, p_t^*, p_{Ht}^*, p_{Ft}^*, q_t, r_t, r_t^*\},$$

given the endogenous state variable b_{t-1}^*, exogenous state variables $\{\beta_t, \beta_t^*, z_t, z_t^*, \gamma_t\}$, and the evolution of exogenous state variables.

A.2 First-order approximation with currency risk premium

We now characterize the first-order approximation employed in the paper. Since the approximation for all equilibrium conditions except arbitrageurs' portfolio choice condition is standard, we focus on the latter here.

The first-order approximations for $\log q_t$, $\log(1 + r_t^*)$, $\log(1 + r_t)$, and b_t^{a*} are

$$\begin{aligned}
\log q_t &= \log q + \boldsymbol{\delta^q} (\boldsymbol{\theta}_t - \boldsymbol{\theta}), \\
\log(1 + r_t^*) &= \log(1 + r^*) + \boldsymbol{\delta^{r^*}} (\boldsymbol{\theta}_t - \boldsymbol{\theta}), \\
\log(1 + r_t) &= \log(1 + r) + \boldsymbol{\delta^r} (\boldsymbol{\theta}_t - \boldsymbol{\theta}), \\
b_t^{a*} &= b^{a*} + \boldsymbol{\delta^{b^{a*}}} (\boldsymbol{\theta}_t - \boldsymbol{\theta}),
\end{aligned}$$

where $\boldsymbol{\delta^x}$ for $x \in \{q, r^*, r, b^{a*}\}$ is a row vector of coefficients on the state variables and $\boldsymbol{\theta}_t$ is the column vector of state variables. The evolution of state variables is given by

$$\boldsymbol{\theta}_t = \boldsymbol{\theta} + \boldsymbol{\Delta^\theta} (\boldsymbol{\theta}_{t-1} - \boldsymbol{\theta}) + \boldsymbol{\delta_\epsilon^\theta} \sigma \boldsymbol{\epsilon}_t,$$

where $\boldsymbol{\Delta^\theta}$ is a matrix of coefficients on lagged state variables, $\boldsymbol{\delta_\epsilon^\theta}$ is a matrix of coefficients on shocks, and $\boldsymbol{\epsilon}_t$ is the column vector of shocks. We scale all shocks by the perturbation parameter σ, and ignore coefficients on this parameter itself anticipating that these will equal zero around the point of approximation.

Now by the property of lognormally distributed variables, it follows that

$$\begin{aligned}
&Var_t \exp\left(-\left[\log q + \boldsymbol{\delta^q} (\boldsymbol{\theta}_{t+1} - \boldsymbol{\theta})\right]\right), \\
&\quad = Var_t \exp\left(-\left[\log q + \boldsymbol{\delta^q \Delta^\theta} (\boldsymbol{\theta}_t - \boldsymbol{\theta}) + \boldsymbol{\delta^q \delta_\epsilon^\theta} \sigma \boldsymbol{\epsilon}_{t+1}\right]\right), \\
&\quad = \exp\left(-2\left[\log q + \boldsymbol{\delta^q \Delta^\theta} (\boldsymbol{\theta}_t - \boldsymbol{\theta})\right]\right) \left(\exp\left(\boldsymbol{\delta^q \delta_\epsilon^\theta} \Sigma \left(\boldsymbol{\delta^q \delta_\epsilon^\theta}\right)' \sigma^2\right) - 1\right) \exp\left(\boldsymbol{\delta^q \delta_\epsilon^\theta} \Sigma \left(\boldsymbol{\delta^q \delta_\epsilon^\theta}\right)' \sigma^2\right),
\end{aligned}$$

where Σ is the covariance matrix of the shocks (scaled appropriately by σ). At the

point of approximation featuring $\sigma \to 0$, let us assume that

$$\gamma(\sigma)\left(\exp\left(\boldsymbol{\delta^q}\boldsymbol{\delta^\theta_\epsilon}\Sigma\left(\boldsymbol{\delta^q}\boldsymbol{\delta^\theta_\epsilon}\right)'\sigma^2\right)-1\right)\to\Gamma$$

for some Γ finite. Then around that point of approximation, substituting the first order approximations for all variables into (9) yields

$$\begin{aligned}&\exp\left(\left(\boldsymbol{\delta^q}-\boldsymbol{\delta^q}\boldsymbol{\Delta^\theta}\right)(\boldsymbol{\theta}_t-\boldsymbol{\theta})+\log(1+r^*)+\boldsymbol{\delta^{r*}}(\boldsymbol{\theta}_t-\boldsymbol{\theta})\right)-\exp\left(\log(1+r)+\boldsymbol{\delta^r}(\boldsymbol{\theta}_t-\boldsymbol{\theta})\right)\\&=\exp\left(\log q+\boldsymbol{\delta^q}(\boldsymbol{\theta}_t-\boldsymbol{\theta})+\log(1+r^*)+\boldsymbol{\delta^{r^*}}(\boldsymbol{\theta}_t-\boldsymbol{\theta})-2\left[\log q+\boldsymbol{\delta^q}\boldsymbol{\Delta^\theta}(\boldsymbol{\theta}_t-\boldsymbol{\theta})\right]+\hat{\gamma}_t\right)\\&\qquad\times\left(b^{a*}+\boldsymbol{\delta^{b^{a*}}}(\boldsymbol{\theta}_t-\boldsymbol{\theta})\right)\Gamma.\end{aligned}$$

Hence, when $\boldsymbol{\theta}_t=\boldsymbol{\theta}$ and $\hat{\gamma}_t=0$ (i.e., at the point of approximation), it must be that

$$(1+r^*)-(1+r)=q^{-1}(1+r^*)b^{a*}\Gamma.$$

Differentiating the above condition with respect to each state variable and evaluating at the point of approximation, the coefficients will solve

$$(1+r^*)(\hat{r}^*_t-\mathbb{E}_t\Delta\hat{q}_{t+1})-(1+r)\hat{r}_t=q^{-1}(1+r^*)b^{a*}\Gamma\left(\hat{q}_t-2\mathbb{E}_t\hat{q}_{t+1}+\hat{r}^*_t+\frac{1}{b^{a*}}\hat{b}^{a*}_t+\hat{\gamma}_t\right),$$

for $\hat{\cdot}$ denoting log/level deviations from the point of approximation. Combining the last two results, we can equivalently write the previous condition as

$$\hat{r}^*_t-\mathbb{E}_t\Delta\hat{q}_{t+1}-\hat{r}_t=\frac{q^{-1}b^{a*}\Gamma}{1-2q^{-1}b^{a^*}\Gamma}\left(\hat{r}_t-\hat{q}_t-\hat{r}^*_t+\frac{1}{b^{a*}}\hat{b}^{a*}_t+\hat{\gamma}_t\right),$$

which is the form stated in the main text and used in the proofs in the next section.

B Proofs

We now provide the proofs of the analytical results described in section 3.

B.1 Log-linearized system and solution around autarkic limit

We first outline the log-linearized equilibrium system and we characterize the solution around the autarkic limit. In the following subsections we use these results to prove

Propositions 1-3.

B.1.1 Log-linearized system

Under assumption A1, log-linearizing (2)-(20) yields:

$$\hat{c}_{Ht} = -\sigma\hat{p}_{Ht} + \hat{c}_t,$$
$$\hat{c}_{Ft} = -\sigma\hat{p}_{Ft} + \hat{c}_t,$$
$$\frac{1}{\psi}\mathbb{E}_t\Delta\hat{c}_{t+1} = \hat{\beta}_t + \hat{r}_t,$$
$$\hat{c}^*_{Ht} = -\sigma\hat{p}^*_{Ht} + \hat{c}^*_t,$$
$$\hat{c}^*_{Ft} = -\sigma\hat{p}^*_{Ft} + \hat{c}^*_t,$$
$$\frac{1}{\psi}\mathbb{E}_t\Delta\hat{c}^*_{t+1} = \hat{\beta}^*_t + \hat{r}^*_t,$$
$$c^*\hat{c}^*_t - \frac{1}{1+r^*}b^*\hat{r}^*_t + \frac{1}{1+r^*}\hat{b}^*_t = c_F\left(\hat{q}_t + \hat{p}_{Ft} + \hat{c}_{Ft}\right) + c^*_F\left(\hat{p}^*_{Ft} + \hat{c}^*_{Ft}\right) + \hat{b}^*_{t-1},$$
$$\hat{r}^*_t - \mathbb{E}_t\Delta\hat{q}_{t+1} - \hat{r}_t = \frac{b^{a*}\Gamma}{1-2b^{a^*}\Gamma}\left(\hat{r}_t - \hat{q}_t - \hat{r}^*_t + \frac{1}{b^{a*}}\hat{b}^{a*}_t + \hat{\gamma}_t\right),$$
$$0 = -\frac{1}{1+r}b^a\hat{r}_t + \frac{1}{1+r}\hat{b}^a_t + \frac{1}{1+r^*}b^{a*}\left(-\hat{q}_t - \hat{r}^*_t\right) + \frac{1}{1+r^*}\hat{b}^{a*}_t,$$
$$\hat{p}_{Ht} = \hat{p}_t,$$
$$-\hat{q}_t + \hat{p}^*_{Ht} = \hat{p}_t,$$
$$\hat{q}_t + \hat{p}_{Ft} = \hat{p}^*_t,$$
$$\hat{p}^*_{Ft} = \hat{p}^*_t,$$
$$0 = \frac{1}{2}(1+\varsigma)\hat{p}_{Ht} + \frac{1}{2}(1-\varsigma)\hat{p}_{Ft},$$
$$0 = \frac{1}{2}(1-\varsigma)\hat{p}^*_{Ht} + \frac{1}{2}(1+\varsigma)\hat{p}^*_{Ft},$$
$$c_H\hat{c}_{Ht} + c^*_H\hat{c}^*_{Ht} = z\hat{z}_t,$$
$$c_F\hat{c}_{Ft} + c^*_F\hat{c}^*_{Ft} = z^*\hat{z}^*_t,$$
$$\hat{b}_t + \hat{b}^a_t = 0,$$
$$\hat{b}^{a*}_t + \hat{b}^*_t = 0.$$

The solution is given by

$$\hat{x}_t = \delta^x_\beta\hat{\beta}_t + \delta^x_{\beta^*}\hat{\beta}^*_t + \delta^x_z\hat{z}_t + \delta^x_{z^*}\hat{z}^*_t + \delta^x_\gamma\hat{\gamma}_t + \delta^x_{b^{a*}}\hat{b}^{a*}_{t-1}$$

for each endogenous variable x and coefficients $\delta_\cdot$. Note that we write this with $\hat{b}^{a*}_{t-1}$ rather than $\hat{b}^{*}_{t-1}$ as an endogenous state variable, but the latter is just the negative of the former by market clearing.

We characterize these coefficients around the autarkic limit. Note that at the limit, there would be no trade in goods, thus no trade in financial assets, and thus a zero currency risk premium. To offset this, we assume that as ς approaches one, the price of risk Γ approaches infinity, so that the ratio $b^{a*}\Gamma$ remains finite. The conditions and comparative statics with respect to Γ described in the main text should thus be understood to refer to this composite term.

For those coefficients which are non-zero in the autarkic limit, we characterize the limit. For those coefficients which are zero in the limit, we characterize their limiting behavior proportional to $1-\varsigma$. Before solving for the coefficients, we combine the above conditions to obtain a simpler system, and we use that in the autarkic limit $c = c^* = z = z^*$ (under assumption A1) to simplify certain coefficients. We do, however, retain some terms multiplied by $1-\varsigma$ so that we can properly characterize the limiting behavior. Finally, without loss of generality we assume $z = 1$.

The domestic Euler equations and arbitrageurs' optimality condition are as above:

$$\frac{1}{\psi}\mathbb{E}_t\Delta\hat{c}_{t+1} = \hat{\beta}_t + \hat{r}_t, \tag{21}$$

$$\frac{1}{\psi}\mathbb{E}_t\Delta\hat{c}^*_{t+1} = \hat{\beta}^*_t + \hat{r}^*_t, \tag{22}$$

$$\hat{r}^*_t - \mathbb{E}_t\Delta\hat{q}_{t+1} - \hat{r}_t = \frac{b^{a*}\Gamma}{1-2b^{a^*}\Gamma}\left(\hat{r}_t - \hat{q}_t - \hat{r}^*_t + \frac{1}{b^{a*}}\hat{b}^{a*}_t + \hat{\gamma}_t\right). \tag{23}$$

Combining Foreign goods market clearing, bond market clearing, and definitions of relative prices with the Foreign resource constraint yields

$$\hat{c}^*_t + \frac{1}{1+r^*}b^{a*}\hat{r}^*_t - \frac{1}{1+r^*}\hat{b}^{a*}_t = -\frac{1}{2}(1-\varsigma)\hat{q}_t + \hat{z}^*_t - \hat{b}^{a*}_{t-1}. \tag{24}$$

Finally, combining households' intratemporal optimality conditions and the definitions of relative prices with the goods market clearing conditions yields

$$-\frac{1}{2}(1+\varsigma)(1-\varsigma)\sigma\hat{q}_t + \frac{1}{2}(1+\varsigma)\hat{c}_t + \frac{1}{2}(1-\varsigma)\hat{c}^*_t = \hat{z}_t, \tag{25}$$

$$\frac{1}{2}(1+\varsigma)(1-\varsigma)\sigma\hat{q}_t + \frac{1}{2}(1-\varsigma)\hat{c}_t + \frac{1}{2}(1+\varsigma)\hat{c}^*_t = \hat{z}^*_t. \tag{26}$$

The system (21)-(26) is 6 equations in 6 unknowns

$$\{\hat{c}_t, \hat{c}_t^*, \hat{b}_t^{a*}, \hat{q}_t, \hat{r}_t, \hat{r}_t^*\}$$

given state variables

$$\{\hat{z}_t, \hat{z}_t^*, \hat{\beta}_t, \hat{\beta}_t^*, \hat{\gamma}_t, \hat{b}_{t-1}^{a*}\}$$

and the evolution of exogenous state variables.

B.1.2 Solution

We now characterize the coefficients $\delta_{\cdot}^{\cdot}$ solving the system (21)-(26) using the method of undetermined coefficients.

Coefficients on $\hat{b}_{t-1}^{a*}$ By the method of undetermined coefficients, these solve

$$\begin{aligned}
&\frac{1}{\psi}\delta_{b^{a*}}^{c}\left(\delta_{b^{a*}}^{b^{a*}}-1\right)=\delta_{b^{a*}}^{r},\\
&\frac{1}{\psi}\delta_{b^{a*}}^{c^*}\left(\delta_{b^{a*}}^{b^{a*}}-1\right)=\delta_{b^{a*}}^{r^*},\\
&\delta_{b^{a*}}^{c^*}+\frac{1}{1+r^*}b^{a*}\delta_{b^{a*}}^{r^*}-\frac{1}{1+r^*}\delta_{b^{a*}}^{b^{a*}}=-\frac{1}{2}\left(1-\varsigma\right)\delta_{b^{a*}}^{q}-1,\\
&\delta_{b^{a*}}^{r^*}-\delta_{b^{a*}}^{q}\left(\delta_{b^{a*}}^{b^{a*}}-1\right)-\delta_{b^{a*}}^{r}=\frac{b^{a^*}\Gamma}{1-2b^{a^*}\Gamma}\left[\delta_{b^{a*}}^{r}-\delta_{b^{a*}}^{q}-\delta_{b^{a*}}^{r^*}+\frac{1}{b^{a*}}\delta_{b^{a*}}^{b^{a*}}\right],\\
&-\frac{1}{2}\left(1+\varsigma\right)\left(1-\varsigma\right)\sigma\delta_{b^{a*}}^{q}+\frac{1}{2}\left(1+\varsigma\right)\delta_{b^{a*}}^{c}+\frac{1}{2}\left(1-\varsigma\right)\delta_{b^{a*}}^{c^*}=0,\\
&\frac{1}{2}\left(1+\varsigma\right)\left(1-\varsigma\right)\sigma\delta_{b^{a*}}^{q}+\frac{1}{2}\left(1-\varsigma\right)\delta_{b^{a*}}^{c}+\frac{1}{2}\left(1+\varsigma\right)\delta_{b^{a*}}^{c^*}=0.
\end{aligned}$$

We conjecture a solution of the form

$$\delta_{b^{a*}}^{q}=\frac{1}{1-\varsigma}\tilde{\delta}_{b^{a*}}^{q}.$$

Substituting these into the previous system and solving yields

$$\begin{aligned}
\delta_{b^{a*}}^{b^{a*}}:=&\frac{2}{2\sigma-1}\left(1-\frac{1}{1+r^*}\delta_{b^{a*}}^{b^{a*}}\right)\left(1-\delta_{b^{a*}}^{b^{a*}}\right)\\
&-\frac{b^{a^*}\Gamma}{1-2b^{a^*}\Gamma}\left(-\frac{2}{2\sigma-1}\left(1-\frac{1}{1+r^*}\delta_{b^{a*}}^{b^{a*}}\right)+\frac{1-\varsigma}{b^{a*}}\delta_{b^{a*}}^{b^{a*}}\right)=0,
\end{aligned}$$

$$\tilde{\delta}^q_{b^{a*}} = \frac{2}{2\sigma - 1}\left(1 - \frac{1}{1+r^*}\delta^{b^{a*}}_{b^{a*}}\right),$$
$$\delta^c_{b^{a*}} = \frac{2\sigma}{2\sigma - 1}\left(1 - \frac{1}{1+r^*}\delta^{b^{a*}}_{b^{a*}}\right),$$
$$\delta^{c^*}_{b^{a*}} = -\frac{2\sigma}{2\sigma - 1}\left(1 - \frac{1}{1+r^*}\delta^{b^{a*}}_{b^{a*}}\right),$$
$$\delta^r_{b^{a*}} = \frac{1}{\psi}\delta^c_{b^{a*}}\left(\delta^{b^{a*}}_{b^{a*}} - 1\right),$$
$$\delta^{r^*}_{b^{a*}} = \frac{1}{\psi}\delta^{c^*}_{b^{a*}}\left(\delta^{b^{a*}}_{b^{a*}} - 1\right).$$

Coefficients on $\hat{\beta}^*_t$, $\hat{\beta}^*_t$, $\hat{z}_t$, $\hat{z}^*_t$, and $\hat{\gamma}_t$ We similarly use the method of undetermined coefficients to characterize the coefficients on the exogenous state variables. For brevity we summarize the solutions here.

On $\hat{\beta}_t$ we obtain:

$$\delta^q_\beta = -\frac{2}{2\sigma-1}\frac{\left(1+\frac{b^{a^*}\Gamma}{1-2b^{a^*}\Gamma}\right)\frac{1}{1+r^*}}{\frac{2}{2\sigma-1}\frac{1}{1+r^*}(1-\rho^\beta)+\tilde{\delta}^q_{b^{a*}}+\frac{b^{a^*}\Gamma}{1-2b^{a^*}\Gamma}\left[\frac{2}{2\sigma-1}\frac{1}{1+r^*}+\frac{1-\varsigma}{b^{a*}}\right]},$$
$$\delta^{b^{a*}}_\beta = (1-\varsigma)\tilde{\delta}^{b^{a*}}_\beta,\ \ \tilde{\delta}^{b^{a*}}_\beta = \frac{1+\frac{b^{a^*}\Gamma}{1-2b^{a^*}\Gamma}}{\frac{2}{2\sigma-1}\frac{1}{1+r^*}(1-\rho^\beta)+\tilde{\delta}^q_{b^{a*}}+\frac{b^{a^*}\Gamma}{1-2b^{a^*}\Gamma}\left[\frac{2}{2\sigma-1}\frac{1}{1+r^*}+\frac{1-\varsigma}{b^{a*}}\right]},$$
$$\delta^c_\beta = (1-\varsigma)\tilde{\delta}^c_\beta,\ \ \tilde{\delta}^c_\beta = -\frac{2\sigma}{2\sigma-1}\frac{1}{1+r^*}\tilde{\delta}^{b^{a*}}_\beta,$$
$$\delta^{c^*}_\beta = (1-\varsigma)\tilde{\delta}^{c^*}_\beta,\ \ \tilde{\delta}^{c^*}_\beta = \frac{2\sigma}{2\sigma-1}\frac{1}{1+r^*}\tilde{\delta}^{b^{a*}}_\beta,$$
$$\delta^r_\beta := -1,$$
$$\delta^{r^*}_\beta = 0,$$

On $\hat{\beta}^*_t$ we obtain:

$$\delta^q_{\beta^*} = -\frac{2}{2\sigma-1}\frac{-\frac{1}{1+r^*}+\frac{1}{1+r^*}\frac{b^{a*}}{1-\varsigma}\tilde{\delta}^q_{b^{a*}}}{\frac{2}{2\sigma-1}\frac{1}{1+r^*}(1-\rho^{\beta^*})+\tilde{\delta}^q_{b^{a*}}+\frac{b^{a^*}\Gamma}{1-2b^{a^*}\Gamma}\left[\frac{2}{2\sigma-1}\frac{1}{1+r^*}+\frac{1-\varsigma}{b^{a*}}\right]},$$
$$\delta^{b^{a*}}_{\beta^*} = (1-\varsigma)\tilde{\delta}^{b^{a*}}_\beta,\ \ \tilde{\delta}^{b^{a*}}_\beta = -\frac{1+\frac{2}{2\sigma-1}\frac{1}{1+r^*}\frac{b^{a*}}{1-\varsigma}(1-\rho^{\beta^*})+\frac{b^{a^*}\Gamma}{1-2b^{a^*}\Gamma}\left[\frac{2}{2\sigma-1}\frac{1}{1+r^*}\frac{b^{a*}}{1-\varsigma}+1\right]}{\frac{2}{2\sigma-1}\frac{1}{1+r^*}(1-\rho^{\beta^*})+\tilde{\delta}^q_{b^{a*}}+\frac{b^{a^*}\Gamma}{1-2b^{a^*}\Gamma}\left[\frac{2}{2\sigma-1}\frac{1}{1+r^*}+\frac{1-\varsigma}{b^{a*}}\right]},$$
$$\delta^c_{\beta^*} = (1-\varsigma)\tilde{\delta}^c_{\beta^*},\ \ \tilde{\delta}^c_{\beta^*} = -\frac{2\sigma}{2\sigma-1}\left(\frac{1}{1+r^*}\frac{b^{a*}}{1-\varsigma}+\frac{1}{1+r^*}\tilde{\delta}^{b^{a*}}_{\beta^*}\right),$$

$$\delta^{c^*}_{\beta^*} = (1-\varsigma)\tilde{\delta}^{c^*}_{\beta^*}, \;\; \tilde{\delta}^{c^*}_{\beta^*} = \frac{2\sigma}{2\sigma-1}\left(\frac{1}{1+r^*}\frac{b^{a*}}{1-\varsigma} + \frac{1}{1+r^*}\tilde{\delta}^{b^{a*}}_{\beta^*}\right),$$

$$\delta^{r}_{\beta^*} = 0,$$

$$\delta^{r^*}_{\beta^*} = -1.$$

On $\hat{z}_t$ we obtain:

$$\delta^{q}_{z} = -\frac{2}{2\sigma-1}\frac{\left(1+\frac{b^{a^*}\Gamma}{1-2b^{a^*}\Gamma}\right)\frac{1}{\psi}\frac{1}{1+r^*}(1-\rho^z) + \frac{1}{2}\tilde{\delta}^{q}_{b^{a*}} + \frac{b^{a^*}\Gamma}{1-2b^{a^*}\Gamma}\frac{\frac{1}{2}(1-\varsigma)}{b^*}}{\frac{2}{2\sigma-1}\frac{1}{1+r^*}(1-\rho^z) + \tilde{\delta}^{q}_{b^{a*}} + \frac{b^{a^*}\Gamma}{1-2b^{a^*}\Gamma}\left[\frac{2}{2\sigma-1}\frac{1}{1+r^*} + \frac{1-\varsigma}{b^{a*}}\right]},$$

$$\delta^{b^{a*}}_{z} = (1-\varsigma)\tilde{\delta}^{b^{a*}}_{z}, \;\; \tilde{\delta}^{b^{a*}}_{z} = \frac{\left(-\frac{1}{2\sigma-1} + \left(1+\frac{b^{a^*}\Gamma}{1-2b^{a^*}\Gamma}\right)\frac{1}{\psi}\right)(1-\rho^z) - \frac{b^{a^*}\Gamma}{1-2b^{a^*}\Gamma}\frac{1}{2\sigma-1}}{\frac{2}{2\sigma-1}\frac{1}{1+r^*}(1-\rho^z) + \tilde{\delta}^{q}_{b^{a*}} + \frac{b^{a^*}\Gamma}{1-2b^{a^*}\Gamma}\left[\frac{2}{2\sigma-1}\frac{1}{1+r^*} + \frac{1-\varsigma}{b^{a*}}\right]},$$

$$\delta^{c}_{z} = 1,$$

$$\delta^{c^*}_{z} = (1-\varsigma)\tilde{\delta}^{c^*}_{z}, \;\; \tilde{\delta}^{c^*}_{z} = \frac{1}{2}\frac{1}{2\sigma-1} + \frac{2\sigma}{2\sigma-1}\frac{1}{1+r^*}\tilde{\delta}^{b^{a*}}_{z},$$

$$\delta^{r}_{z} = -\frac{1}{\psi}(1-\rho^z),$$

$$\delta^{r^*}_{z} = 0.$$

On $\hat{z}^*_t$ we obtain:

$$\delta^{q}_{z^*} = \frac{2}{2\sigma-1}\frac{\frac{1}{\psi}\frac{1}{1+r^*}(1-\rho^{z^*}) + \left(\frac{1}{2} - \frac{1}{1+r^*}\frac{b^{a*}}{1-\varsigma}\frac{1}{\psi}\left(1-\rho^{z^*}\right)\right)\tilde{\delta}^{q}_{b^{a*}} + \frac{b^{a^*}\Gamma}{1-2b^{a^*}\Gamma}\frac{\frac{1}{2}(1-\varsigma)}{b^{a*}}}{\frac{2}{2\sigma-1}\frac{1}{1+r^*}(1-\rho^{z^*}) + \tilde{\delta}^{q}_{b^{a*}} + \frac{b^{a^*}\Gamma}{1-2b^{a^*}\Gamma}\left[\frac{2}{2\sigma-1}\frac{1}{1+r^*} + \frac{1-\varsigma}{b^{a*}}\right]},$$

$$\delta^{b^{a*}}_{z^*} = 2\left[\frac{\left(\frac{2}{2\sigma-1}\left(\frac{1}{2} - \frac{1}{1+r^*}\frac{b^{a*}}{1-\varsigma}\frac{1}{\psi}\left(1-\rho^{z^*}\right)\right) - \frac{1}{\psi}\right)(1-\rho^{z^*})}{\frac{2}{2\sigma-1}\frac{1}{1+r^*}(1-\rho^{z^*}) + \tilde{\delta}^{q}_{b^{a*}} + \frac{b^{a^*}\Gamma}{1-2b^{a^*}\Gamma}\left[\frac{2}{2\sigma-1}\frac{1}{1+r^*} + \frac{1-\varsigma}{b^{a*}}\right]}\right.$$

$$\left. + \frac{\frac{b^{a^*}\Gamma}{1-2b^{a^*}\Gamma}\left[\frac{2}{2\sigma-1}\left(\frac{1}{2} - \frac{1}{1+r^*}\frac{b^{a*}}{1-\varsigma}\frac{1}{\psi}\left(1-\rho^{z^*}\right)\right) - \frac{1}{\psi}(1-\rho^{z^*})\right]}{\frac{2}{2\sigma-1}\frac{1}{1+r^*}(1-\rho^{z^*}) + \tilde{\delta}^{q}_{b^{a*}} + \frac{b^{a^*}\Gamma}{1-2b^{a^*}\Gamma}\left[\frac{2}{2\sigma-1}\frac{1}{1+r^*} + \frac{1-\varsigma}{b^{a*}}\right]}\right],$$

$$\delta^{c}_{z^*} = (1-\varsigma)\tilde{\delta}^{c}_{z^*}, \;\; \tilde{\delta}^{c}_{z^*} = \frac{1}{2}\frac{1}{2\sigma-1} - \frac{2\sigma}{2\sigma-1}\left(\frac{1}{1+r^*}\frac{b^{a*}}{1-\varsigma}\frac{1}{\psi}\left(1-\rho^{z^*}\right) + \frac{1}{1+r^*}\tilde{\delta}^{b^{a*}}_{z^*}\right),$$

$$\delta^{c^*}_{z^*} = 1,$$

$$\delta^{r}_{z^*} = 0,$$

$$\delta_{z^*}^{r^*} = -\frac{1}{\psi}(1-\rho^{z^*}).$$

Finally, on $\hat{\gamma}_t$ we obtain:

$$\delta_{\gamma}^{q} = \frac{\frac{b^{a^*}\Gamma}{1-2b^{a^*}\Gamma}\frac{2}{2\sigma-1}\frac{1}{1+r^*}}{\frac{2}{2\sigma-1}\frac{1}{1+r^*}(1-\rho^{\gamma}) + \tilde{\delta}_{b^{a*}}^{q} + \frac{b^{a^*}\Gamma}{1-2b^{a^*}\Gamma}\left[\frac{2}{2\sigma-1}\frac{1}{1+r^*} + \frac{1-\varsigma}{b^{a*}}\right]},$$

$$\delta_{\gamma}^{b^{a*}} = (1-\varsigma)\tilde{\delta}_{\gamma}^{b^{a*}}, \;\; \tilde{\delta}_{\gamma}^{b^{a*}} = -\frac{\frac{b^{a^*}\Gamma}{1-2b^{a^*}\Gamma}}{\frac{2}{2\sigma-1}\frac{1}{1+r^*}(1-\rho^{\gamma}) + \tilde{\delta}_{b^{a*}}^{q} + \frac{b^{a^*}\Gamma}{1-2b^{a^*}\Gamma}\left[\frac{2}{2\sigma-1}\frac{1}{1+r^*} + \frac{1-\varsigma}{b^{a*}}\right]},$$

$$\delta_{\gamma}^{c} = (1-\varsigma)\tilde{\delta}_{\gamma}^{c}, \;\; \tilde{\delta}_{\gamma}^{c} = -\frac{2\sigma}{2\sigma-1}\frac{1}{1+r^*}\tilde{\delta}_{\gamma}^{b^{a*}},$$

$$\delta_{\gamma}^{c^*} = (1-\varsigma)\tilde{\delta}_{\gamma}^{c^*}, \;\; \tilde{\delta}_{\gamma}^{c^*} = \frac{2\sigma}{2\sigma-1}\frac{1}{1+r^*}\tilde{\delta}_{\gamma}^{b^{a*}},$$

$$\delta_{\gamma}^{r} = (1-\varsigma)\tilde{\delta}_{\gamma}^{r}, \;\; \tilde{\delta}_{\gamma}^{r} = \frac{1}{\psi}\left(\tilde{\delta}_{\gamma}^{c}(\rho^{\gamma}-1) + \delta_{b^{a*}}^{c}\tilde{\delta}_{\gamma}^{b^{a*}}\right),$$

$$\delta_{\gamma}^{r^*} = (1-\varsigma)\tilde{\delta}_{\gamma}^{r^*}, \;\; \tilde{\delta}_{\gamma}^{r^*} = \frac{1}{\psi}\left(\tilde{\delta}_{\gamma}^{c^*}(\rho^{\gamma}-1) + \delta_{b^{a*}}^{c^*}\tilde{\delta}_{\gamma}^{b^{a*}}\right).$$

We repeatedly reference these coefficients in the proofs of Propositions 1-3 which follow.

B.2 Proposition 1

Proof. Let us first characterize $\hat{q}_t$ given a single driving force $x \in \{\beta, \beta^*, z, z^*, \gamma\}$. We have

$$\begin{aligned}
\hat{q}_t &= \delta_x^q \hat{x}_t + \delta_{b^{a*}}^q \hat{b}_{t-1}^{a*}, \\
&= \delta_x^q \hat{\epsilon}_t^x + \sum_{\tau=0}^{\infty}\left[\delta_x^q (\rho^x)^{\tau+1} + \delta_{b^{a*}}^q \delta_x^{b^{a*}} \frac{(\rho^x)^{\tau+1} - \left(\delta_{b^{a*}}^{b^{a*}}\right)^{\tau+1}}{\rho^x - \delta_{b^{a*}}^{b^{a*}}}\right]\hat{\epsilon}_{t-1-\tau}^x, \\
&= \delta_x^q \hat{\epsilon}_t^x + \sum_{\tau=0}^{\infty}\left[\delta_x^q (\rho^x)^{\tau+1} + \tilde{\delta}_{b^{a*}}^q \tilde{\delta}_x^{b^{a*}} \frac{(\rho^x)^{\tau+1} - \left(\delta_{b^{a*}}^{b^{a*}}\right)^{\tau+1}}{\rho^x - \delta_{b^{a*}}^{b^{a*}}}\right]\hat{\epsilon}_{t-1-\tau}^x.
\end{aligned}$$

Interest rate differential We now characterize the contemporaneous comovements with the interest rate differential $\hat{r}_t^* - \hat{r}_t$.

We begin with β_t shocks (an analogous argument holds for β_t^* shocks). Based on

the results in section B.1.2, in the autarkic limit

$$\begin{aligned}\hat{r}_t^* - \hat{r}_t &= \hat{\beta}_t, \\ &= \sum_{\tau=0}^{\infty} \left(\rho^\beta\right)^\tau \hat{\epsilon}_{t-\tau}^\beta.\end{aligned}$$

Thus, for ς close to one, we have that

$$\begin{aligned}Cov(\hat{q}_t, \hat{r}_t^* - \hat{r}_t) / \left(\sigma^\beta\right)^2 &\approx \sum_{\tau=0}^{\infty} \left[\delta_\beta^q \left(\rho^\beta\right)^\tau + \tilde{\delta}_{b^{a*}}^q \tilde{\delta}_\beta^{b^{a*}} \frac{\left(\rho^\beta\right)^\tau - \left(\delta_{b^{a*}}^{b^{a*}}\right)^\tau}{\rho^\beta - \delta_{b^{a*}}^{b^{a*}}}\right] \left(\rho^\beta\right)^\tau, \\ &= \frac{1}{1-\left(\rho^\beta\right)^2} \frac{1}{1-\rho^\beta \delta_{b^{a*}}^{b^{a*}}} \left[\delta_\beta^q \left(1-\rho^\beta \delta_{b^{a*}}^{b^{a*}}\right) + \tilde{\delta}_{b^{a*}}^q \tilde{\delta}_\beta^{b^{a*}} \rho^\beta\right],\end{aligned}$$

where the second line follows from straightforward algebra. As $\Gamma \to 0$ and thus $\delta_{b^{a*}}^{b^{a*}} \to 1$, at the autarkic limit the expression in brackets is

$$\begin{aligned}\delta_\beta^q \left(1-\rho^\beta\right) + \tilde{\delta}_{b^{a*}}^q \tilde{\delta}_\beta^{b^{a*}} \rho^\beta &= -\frac{1-\rho^\beta}{1+r^*-\rho^\beta} + \frac{r^* \rho^\beta}{1+r^*-\rho^\beta}, \\ &= -\frac{1-(1+r^*)\rho^\beta}{1+r^*-\rho^\beta},\end{aligned}$$

using the coefficients characterized in section B.1.2. The numerator reflects two terms. On impact, an increase in U.S. demand appreciates the dollar and lowers the Foreign interest rate relative to the U.S. interest rate, driving a negative correlation. Going forward, the dollar is expected to depreciate, and in the medium run, the increased wealth in Foreign (due to its higher saving) would imply a weak dollar while the U.S. interest rate remains relatively high. Provided r^* is sufficiently small, for any $\rho^\beta < 1$ the former effect will dominate the latter and this comovement will be negative. By continuity, this result also holds away for the autarkic limit and for Γ small. We employ similar arguments for all other comovements.

In particular, next consider z_t shocks (an analogous argument holds for z_t^* shocks). In response to z_t shocks, we have at the autarkic limit

$$\begin{aligned}\hat{r}_t^* - \hat{r}_t &= \frac{1}{\psi}(1-\rho^z)\hat{z}_t, \\ &= \frac{1}{\psi}(1-\rho^z) \sum_{\tau=0}^{\infty} \left(\rho^z\right)^\tau \hat{\epsilon}_{t-\tau}^z.\end{aligned}$$

Using similar steps as above, it follows that as $\Gamma \to 0$ and thus $\delta_{b^{a*}}^{b^{a*}} \to 1$, in the autarkic limit

$$Cov(\hat{q}_t, \hat{r}_t^* - \hat{r}_t) / \left(\sigma^z\right)^2 \propto -(1 - (1 + r^*)\rho^z).$$

Again this will be negative for r^* sufficiently small, given any $\rho^z < 1$.

We finally consider γ_t shocks. We have that

$$\begin{aligned}
\hat{r}_t^* - \hat{r}_t &= \left(\delta_\gamma^{r^*} - \delta_\gamma^r\right) \hat{\gamma}_t + \left(\delta_{b^{a*}}^{r^*} - \delta_{b^{a*}}^r\right) \hat{b}_{t-1}^{a*}, \\
&= \left(\delta_\gamma^{r^*} - \delta_\gamma^r\right) \hat{\epsilon}_t^\gamma + \sum_{\tau=0}^{\infty} \left[\left(\delta_\gamma^{r^*} - \delta_\gamma^r\right) (\rho^\gamma)^{\tau+1} + \left(\delta_{b^{a*}}^{r^*} - \delta_{b^{a*}}^r\right) \delta_\gamma^{b^{a*}} \frac{(\rho^\gamma)^{\tau+1} - \left(\delta_{b^{a*}}^{b^{a*}}\right)^{\tau+1}}{\rho^\gamma - \delta_{b^{a*}}^{b^{a*}}} \right] \hat{\epsilon}_{t-1-\tau}^\gamma.
\end{aligned}$$

Further note that

$$\begin{aligned}
\delta_\gamma^{r^*} &= -\delta_\gamma^r, \\
\delta_{b^{a*}}^{r^*} &= -\delta_{b^{a*}}^r,
\end{aligned}$$

so we can write the above as

$$\hat{r}_t^* - \hat{r}_t = 2\delta_\gamma^{r^*} \hat{\epsilon}_t^\gamma + \sum_{\tau=0}^{\infty} \left[2\delta_\gamma^{r^*} (\rho^\gamma)^{\tau+1} + 2\delta_{b^{a*}}^{r^*} \delta_\gamma^{b^{a*}} \frac{(\rho^\gamma)^{\tau+1} - \left(\delta_{b^{a*}}^{b^{a*}}\right)^{\tau+1}}{\rho^\gamma - \delta_{b^{a*}}^{b^{a*}}} \right] \hat{\epsilon}_{t-1-\tau}^\gamma.$$

Thus, we have that

$$\begin{aligned}
&Cov(\hat{q}_t, \hat{r}_t^* - \hat{r}_t) / \left(2\left(\sigma^\gamma\right)^2\right) \\
&= \sum_{\tau=0}^{\infty} \left[\delta_\gamma^q (\rho^\gamma)^\tau + \tilde{\delta}_{b^{a*}}^q \tilde{\delta}_\gamma^{b^{a*}} \frac{(\rho^\gamma)^\tau - \left(\delta_{b^{a*}}^{b^{a*}}\right)^\tau}{\rho^\gamma - \delta_{b^{a*}}^{b^{a*}}} \right] \left[\delta_\gamma^{r^*} (\rho^\gamma)^\tau + \delta_{b^{a*}}^{r^*} \delta_\gamma^{b^{a*}} \frac{(\rho^\gamma)^\tau - \left(\delta_{b^{a*}}^{b^{a*}}\right)^\tau}{\rho^\gamma - \delta_{b^{a*}}^{b^{a*}}} \right], \\
&= \frac{1}{1 - (\rho^\gamma)^2} \left[\delta_\gamma^q + \tilde{\delta}_{b^{a*}}^q \tilde{\delta}_\gamma^{b^{a*}} \frac{\rho^\gamma}{1 - \left(\rho^\gamma \delta_{b^{a*}}^{b^{a*}}\right)} \right] \delta_\gamma^{r^*} \\
&\quad + \frac{1}{1 - (\rho^\gamma)^2} \left[\delta_\gamma^q + \tilde{\delta}_{b^{a*}}^q \tilde{\delta}_\gamma^{b^{a*}} \frac{\rho^\gamma}{1 - \left(\rho^\gamma \delta_{b^{a*}}^{b^{a*}}\right)} \right] \delta_{b^{a*}}^{r^*} \delta_\gamma^{b^{a*}} \frac{1}{\rho^\gamma - \delta_{b^{a*}}^{b^{a*}}} \\
&\quad - \frac{1}{1 - \rho^\gamma \delta_{b^{a*}}^{b^{a*}}} \left[\delta_\gamma^q + \tilde{\delta}_{b^{a*}}^q \tilde{\delta}_\gamma^{b^{a*}} \frac{\delta_{b^{a*}}^{b^{a*}}}{1 - \left(\delta_{b^{a*}}^{b^{a*}}\right)^2} \right] \delta_{b^{a*}}^{r^*} \delta_\gamma^{b^{a*}} \frac{1}{\rho^\gamma - \delta_{b^{a*}}^{b^{a*}}},
\end{aligned}$$

where the last line follows from straightforward algebra.

Now since

$$\delta_{b^{a*}}^{r^*} = \frac{1}{\psi}\delta_{b^{a*}}^{c^*}\left(\delta_{b^{a*}}^{b^{a*}} - 1\right),$$

we can write this as

$$\begin{aligned}
&Cov(\hat{q}_t, \hat{r}_t^* - \hat{r}_t)/\left(2\left(\sigma^\gamma\right)^2\right) \\
&\quad= \frac{1}{1-\left(\rho^\gamma\right)^2}\left[\delta_\gamma^q + \tilde{\delta}_{b^{a*}}^q\tilde{\delta}_\gamma^{b^{a*}}\frac{\rho^\gamma}{1-\left(\rho^\gamma\delta_{b^{a*}}^{b^{a*}}\right)}\right]\delta_\gamma^{r^*} \\
&\quad+ \frac{1}{1-\left(\rho^\gamma\right)^2}\left[\delta_\gamma^q + \tilde{\delta}_{b^{a*}}^q\tilde{\delta}_\gamma^{b^{a*}}\frac{\rho^\gamma}{1-\left(\rho^\gamma\delta_{b^{a*}}^{b^{a*}}\right)}\right]\delta_{b^{a*}}^{r^*}\delta_\gamma^{b^{a*}}\frac{1}{\rho^\gamma - \delta_{b^{a*}}^{b^{a*}}} \\
&\quad- \frac{1}{1-\rho^\gamma\delta_{b^{a*}}^{b^{a*}}}\left[\delta_\gamma^q\right]\delta_{b^{a*}}^{r^*}\delta_\gamma^{b^{a*}}\frac{1}{\rho^\gamma - \delta_{b^{a*}}^{b^{a*}}} \\
&\quad+ \frac{1}{1-\rho^\gamma\delta_{b^{a*}}^{b^{a*}}}\tilde{\delta}_{b^{a*}}^q\tilde{\delta}_\gamma^{b^{a*}}\frac{\delta_{b^{a*}}^{b^{a*}}}{1+\delta_{b^{a*}}^{b^{a*}}}\frac{1}{\psi}\delta_{b^{a*}}^{c^*}\delta_\gamma^{b^{a*}}\frac{1}{\rho^\gamma - \delta_{b^{a*}}^{b^{a*}}}.
\end{aligned}$$

As $\Gamma \to 0$, we have that $\delta_{b^{a*}}^{r^*} \to 0$, so we focus on the first and last terms alone. Substituting in the values of the other coefficients as $\Gamma \to 0$ and again focusing on the case with r^* small, we have that the sign of $Cov(\hat{q}_t, \hat{r}_t^* - \hat{r}_t)/(2(\sigma^\gamma)^2)$ is governed by the impact effect of the shock $(\delta_\gamma^q\delta_\gamma^{r^*})$, which implies a positive comovement.

Lagged interest rate differential We now characterize the comovements with the lagged interest rate differential $\hat{r}_{t-1}^* - \hat{r}_{t-1}$, reflected in the Fama (1984) regression coefficient.

In response to β_t shocks, we already prove in Proposition 3 that $Cov(\Delta\hat{q}_{t+1}, \hat{r}_t^* - \hat{r}_t)/\left(\sigma^\beta\right)^2 > 0$.

In response to z_t shocks, the same steps as in the proof of Proposition 3 imply

$$Cov(\Delta\hat{q}_{t+1}, \hat{r}_t^* - \hat{r}_t)/\left(\sigma^z\right)^2 \propto -\delta_z^q + \tilde{\delta}_{b^{a*}}^q\tilde{\delta}_z^{b^{a*}}\frac{1}{1-\delta_{b^{a*}}^{b^{a*}}\rho^z}.$$

For $\Gamma \to 0$, this is positive.

Finally, in response to γ_t shocks, for r^* small we similarly have

$$Cov(\Delta\hat{q}_{t+1}, \hat{r}_t^* - \hat{r}_t)/\left(\sigma^\gamma\right)^2 \propto -\delta_\gamma^{r^*}\delta_\gamma^q,$$

which is negative.

Consumption differential Let us start with z_t shocks, since it is clear that in the autarkic limit $\hat{c}_t^* - \hat{c}_t = \hat{z}_t^* - \hat{z}_t$. We have that

$$\hat{z}_t^* - \hat{z}_t = \sum_{\tau=0}^{\infty} \left(\rho^{z^*}\right)^{\tau} \hat{\epsilon}_{t-\tau}^{z^*} - \sum_{\tau=0}^{\infty} \left(\rho^{z}\right)^{\tau} \hat{\epsilon}_{t-\tau}^{z}.$$

Thus, using similar steps as above, in response to z_t shocks we have that as $\Gamma \to 0$

$$Cov(\hat{q}_t, \hat{z}_t^* - \hat{z}_t)/\sigma^2 \propto 1 - (1 + r^*)\rho^z,$$

which is positive for r^* sufficiently small, given any $\rho^z < 1$.

Now let us focus on β_t and γ_t shocks. For $x \in \{\beta, \gamma\}$, we have that

$$\begin{aligned}
&\hat{c}_t^* - \hat{c}_t \\
&= \left(\delta_x^{c^*} - \delta_x^c\right) \hat{\epsilon}_t^x + \sum_{\tau=0}^{\infty} \left[\left(\delta_x^{c^*} - \delta_x^c\right) \left(\rho^x\right)^{\tau+1} + \left(\delta_{b^{a*}}^{c^*} - \delta_{b^{a*}}^c\right) \delta_x^{b^{a*}} \frac{\left(\rho^x\right)^{\tau+1} - \left(\delta_{b^{a*}}^{b^{a*}}\right)^{\tau+1}}{\rho^x - \delta_{b^{a*}}^{b^{a*}}} \right] \hat{\epsilon}_{t-1-\tau}^x.
\end{aligned}$$

Note that

$$\begin{aligned}
\delta_{b^{a*}}^c &= -\delta_{b^{a*}}^{c^*}, \\
\delta_\beta^c &= -\delta_\beta^{c^*}, \\
\delta_\gamma^c &= -\delta_\gamma^{c^*}.
\end{aligned}$$

Hence, we have that

$$\hat{c}_t^* - \hat{c}_t = 2\delta_x^{c^*} \hat{\epsilon}_t^x + \sum_{\tau=0}^{\infty} \left[2\delta_x^{c^*} \left(\rho^x\right)^{\tau+1} + 2\delta_{b^{a*}}^{c^*} \delta_x^{b^{a*}} \frac{\left(\rho^x\right)^{\tau+1} - \left(\delta_{b^{a*}}^{b^{a*}}\right)^{\tau+1}}{\rho^x - \delta_{b^{a*}}^{b^{a*}}} \right] \hat{\epsilon}_{t-1-\tau}^x.$$

Now consider β_t shocks in particular. Using similar steps as above, it follows that

$$\begin{aligned}
&Cov(\hat{q}_t, \hat{c}_t^* - \hat{\tilde{c}}_t) / \left(2\left(\sigma^\beta\right)^2\right) \\
&\quad = \sum_{\tau=0}^{\infty} \left[\delta_\beta^q \left(\rho^\beta\right)^{\tau} + \tilde{\delta}_{b^{a*}}^q \tilde{\delta}_\beta^{b^{a*}} \frac{\left(\rho^\beta\right)^{\tau} - \left(\delta_{b^{a*}}^{b^{a*}}\right)^{\tau}}{\rho^\beta - \delta_{b^{a*}}^{b^{a*}}} \right] \left[\delta_\beta^{c^*} \left(\rho^\beta\right)^{\tau} + \delta_{b^{a*}}^{c^*} \delta_\beta^{b^{a*}} \frac{\left(\rho^\beta\right)^{\tau} - \left(\delta_{b^{a*}}^{b^{a*}}\right)^{\tau}}{\rho^\beta - \delta_{b^{a*}}^{b^{a*}}} \right], \\
&\quad = \frac{1}{1 - \left(\rho^\beta\right)^2} \left[\delta_\beta^q + \tilde{\delta}_{b^{a*}}^q \tilde{\delta}_\beta^{b^{a*}} \frac{\rho^\beta}{1 - \left(\rho^\beta \delta_{b^{a*}}^{b^{a*}}\right)} \right] \delta_\beta^{c^*}
\end{aligned}$$

$$+\frac{1}{1-(\rho^{\beta})^{2}}\left[\delta_{\beta}^{q}+\tilde{\delta}_{b^{a*}}^{q}\tilde{\delta}_{\beta}^{b^{a*}}\frac{\rho^{\beta}}{1-\left(\rho^{\beta}\delta_{b^{a*}}^{b^{a*}}\right)}\right]\delta_{b^{a*}}^{c^{*}}\delta_{\beta}^{b^{a*}}\frac{1}{\rho^{\beta}-\delta_{b^{a*}}^{b^{a*}}}$$
$$-\frac{1}{1-\rho^{\beta}\delta_{b^{a*}}^{b^{a*}}}\left[\delta_{\beta}^{q}+\tilde{\delta}_{b^{a*}}^{q}\tilde{\delta}_{\beta}^{b^{a*}}\frac{\delta_{b^{a*}}^{b^{a*}}}{1-\left(\delta_{b^{a*}}^{b^{a*}}\right)^{2}}\right]\delta_{b^{a*}}^{c^{*}}\delta_{\beta}^{b^{a*}}\frac{1}{\rho^{\beta}-\delta_{b^{a*}}^{b^{a*}}}.$$

As $\Gamma \to 0$, terms multiplying $\delta_{\beta}^{b^{a*}}$ are of order r^* and can be ignored for r^* small. Note that this also includes

$$\frac{\delta_{\beta}^{b^{a*}}}{1-\left(\delta_{b^{a*}}^{b^{a*}}\right)^{2}}$$

in the last term. Recall that

$$\delta_{b^{a*}}^{b^{a*}} := \frac{2}{2\sigma-1}\left(1-\frac{1}{1+r^*}\delta_{b^{a*}}^{b^{a*}}\right)\left(1-\delta_{b^{a*}}^{b^{a*}}\right)$$
$$-\frac{b^{a^*}\Gamma}{1-2b^{a^*}\Gamma}\left(-\frac{2}{2\sigma-1}\left(1-\frac{1}{1+r^*}\delta_{b^{a*}}^{b^{a*}}\right)+\frac{1-\varsigma}{b^{a*}}\delta_{b^{a*}}^{b^{a*}}\right)=0.$$

It follows that around $\Gamma = 0$ (which implies $\delta_{b^{a*}}^{b^{a*}} = 1$) and $r^* = 0$,

$$\frac{1-\delta_{b^{a*}}^{b^{a*}}}{r^*} \propto \frac{\Gamma}{(r^*)^2}.$$

In other words

$$\frac{r^*}{1-\delta_{b^{a*}}^{b^{a*}}} \propto \frac{(r^*)^2}{\Gamma}.$$

Hence, if r^* and Γ go to zero at the same rate,

$$\frac{r^*}{1-\left(\delta_{b^{a*}}^{b^{a*}}\right)^{2}} \to 0.$$

It follows that the sign of $Cov(\hat{q}_t, \hat{c}_t^* - \hat{c}_t)/(2(\sigma^{\beta})^2)$ is dominated by $\delta_{\beta}^{q}\delta_{\beta}^{c^*}$, which again reflects the impact effect of a β_t innovation. For small Γ, this is negative.

The same argument applies for γ_t shocks. □

B.3 Proposition 2

Proof. We again evaluate the coefficients characterized in section B.1.2 in the autarkic limit.

The impact effect on the U.S. real interest rate is

$$\delta_\beta^r = -1.$$

The impact effect on the real exchange rate is

$$\delta_\beta^q = -\frac{2}{2\sigma-1}\frac{\left(1+\frac{b^{a^*}\Gamma}{1-2b^{a^*}\Gamma}\right)\frac{1}{1+r^*}}{\frac{2}{2\sigma-1}\frac{1}{1+r^*}(1-\rho^\beta)+\tilde{\delta}^q_{b^{a*}}+\frac{b^{a^*}\Gamma}{1-2b^{a^*}\Gamma}\left[\frac{2}{2\sigma-1}\frac{1}{1+r^*}+\frac{1-\varsigma}{b^{a*}}\right]}.$$

Then, as $\Gamma \to 0$, we have that

$$\delta_\beta^q \to -\frac{1}{1+r^*-\rho^\beta}.$$

It is immediate that this is increasing in absolute magnitude as ρ^β rises.

It is clear from all other coefficients characterized in section B.1.2 that the impact effect on other variables is zero in the autarkic limit.

We now characterize $Var(\mathbb{E}_t\Delta\hat{q}_{t+1})/Var(\Delta\hat{q}_{t+1})$, the share of variance in exchange rate innovations that is accounted for the predictable part. In the autarkic limit and with $\Gamma \to 0$, we have that

$$\mathbb{E}_t\Delta\hat{q}_{t+1} = \hat{r}_t^* - \hat{r}_t = \hat{\beta}_t - \hat{\beta}_t^*,$$

and

$$\Delta\hat{q}_{t+1} = (\Delta\hat{q}_{t+1} - \mathbb{E}_t\Delta\hat{q}_{t+1}) + \mathbb{E}_t\Delta\hat{q}_{t+1} = \delta_\beta^q\hat{\epsilon}_{t+1}^\beta + \delta_{\beta^*}^q\hat{\epsilon}_{t+1}^{\beta^*} + \hat{\beta}_t - \hat{\beta}_t^*.$$

Focusing on β_t shocks alone for simplicity (equivalently, β_t/β_t^* shocks), it follows that

$$\begin{aligned}
Var(\hat{\beta}_t) &= \frac{1}{1-\left(\rho^\beta\right)^2}\left(\sigma^\beta\right)^2, \\
Var(\delta_\beta^q\hat{\epsilon}_t^\beta) &= \left(\frac{1}{1+r^*-\rho^\beta}\right)^2\left(\sigma^\beta\right)^2, \\
Var(\mathbb{E}_t\Delta\hat{q}_{t+1})/Var(\Delta\hat{q}_{t+1}) &= \frac{\frac{1}{1-\left(\rho^\beta\right)^2}\left(\sigma^\beta\right)^2}{\left(\frac{1}{1+r^*-\rho^\beta}\right)^2\left(\sigma^\beta\right)^2+\frac{1}{1-\left(\rho^\beta\right)^2}\left(\sigma^\beta\right)^2}, \\
&= \frac{1}{1+\frac{1-(\rho^\beta)^2}{(1+r^*-\rho^\beta)^2}}.
\end{aligned}$$

If $r^* = 0$, note that this becomes

$$\frac{1}{1+\frac{1+\rho^\beta}{1-\rho^\beta}}.$$

The comparative statics with respect to ρ^β are then immediate. □

B.4 Proposition 3

Proof. We again reference the coefficients characterized in section B.1.2 in the autarkic limit.

Let us first characterize the comparative static of δ^q_β with respect to Γ. First note that

$$\begin{aligned}\frac{1}{b^{a*}}\frac{d\delta^q_\beta}{d\Gamma}|_{\Gamma=0} \propto & -\left[\frac{2}{2\sigma-1}\frac{1}{1+r^*}(1-\rho^\beta)+\frac{2}{2\sigma-1}\frac{r^*}{1+r^*}\right] \\ & + \frac{1}{b^{a*}}\frac{d\tilde{\delta}^q_{b^{a*}}}{d\Gamma}|_{\Gamma=0}+\left[\frac{2}{2\sigma-1}\frac{1}{1+r^*}+\frac{1-\varsigma}{b^{a*}}\right], \\ & = \frac{2}{2\sigma-1}\frac{1}{1+r^*}\rho^\beta - \frac{2}{2\sigma-1}\frac{r^*}{1+r^*}+\frac{1-\varsigma}{b^{a*}}+\frac{1}{b^{a*}}\frac{d\tilde{\delta}^q_{b^{a*}}}{d\Gamma}|_{\Gamma=0}.\end{aligned}$$

The condition defining $\tilde{\delta}^q_{b^{a*}}$ implies

$$\frac{d\tilde{\delta}^q_{b^{a*}}}{d\Gamma}|_{\Gamma=0} = -\frac{2}{2\sigma-1}\frac{1}{1+r^*}\frac{d\delta^{b^{a*}}_{b^{a*}}}{d\Gamma}|_{\Gamma=0}.$$

Finally, implicitly differentiating the condition defining $\delta^{b^{a*}}_{b^{a*}}$ yields

$$-\frac{2}{2\sigma-1}\frac{r^*}{1+r^*}\frac{d\delta^{b^{a*}}_{b^{a*}}}{d\Gamma}|_{\Gamma=0} - b^{a*}\left(-\frac{2}{2\sigma-1}\frac{r^*}{1+r^*}+\frac{1-\varsigma}{b^{a*}}\right)=0.$$

It follows that

$$\frac{d\delta^{b^{a*}}_{b^{a*}}}{d\Gamma}|_{\Gamma=0} = -\frac{1}{\frac{2}{2\sigma-1}\frac{r^*}{1+r^*}}b^{a*}\left(-\frac{2}{2\sigma-1}\frac{r^*}{1+r^*}+\frac{1-\varsigma}{b^{a*}}\right),$$

so

$$\frac{d\tilde{\delta}^q_{b^{a*}}}{d\Gamma}|_{\Gamma=0} = \frac{1}{r^*}b^{a*}\left(-\frac{2}{2\sigma-1}\frac{r^*}{1+r^*}+\frac{1-\varsigma}{b^{a*}}\right).$$

Thus, for r^* small we have that

$$\frac{d\delta_\beta^q}{d\Gamma}|_{\Gamma=0} \propto b^{a*}\frac{1-\varsigma}{b^{a*}} > 0.$$

Recalling that $\delta_\beta^q < 0$ around the autarkic limit, it follows that an increase in Γ dampens the magnitude of the exchange rate response upon a $\hat{\epsilon}_t^\beta$ innovation. For instance, it reduces the magnitude of the dollar appreciation upon a negative $\hat{\epsilon}_t^\beta$ innovation.

The impact effect on the expected carry trade return in the autarkic limit is

$$\frac{b^{a*}\Gamma}{1-2b^{a*}\Gamma}\left[\delta_\beta^r - \delta_\beta^q - \delta_\beta^{r*} + \frac{1-\varsigma}{b^{a*}}\tilde{\delta}_\beta^{b^{a*}}\right] = \frac{b^{a^*}\Gamma}{1-2b^{a^*}\Gamma}\frac{\frac{2}{2\sigma-1}\frac{1}{1+r^*}\rho^\beta - \tilde{\delta}_{b^{a*}}^q + \frac{1-\varsigma}{b^{a*}}}{\frac{2}{2\sigma-1}\frac{1}{1+r^*}(1-\rho^\beta) + \tilde{\delta}_{b^{a*}}^q + \frac{b^{a^*}\Gamma}{1-2b^{a^*}\Gamma}\left[\frac{2}{2\sigma-1}\frac{1}{1+r^*} + \frac{1-\varsigma}{b^{a*}}\right]}.$$

The impact effect on the expected dollar appreciation in the autarkic limit is

$$-\delta_\beta^r - \frac{b^{a*}\Gamma}{1-2b^{a*}\Gamma}\left[\delta_\beta^r - \delta_\beta^q - \delta_\beta^{r*} + \frac{1-\varsigma}{b^{a*}}\tilde{\delta}_\beta^{b^{a*}}\right] = 1 - \frac{b^{a^*}\Gamma}{1-2b^{a^*}\Gamma}\frac{\frac{2}{2\sigma-1}\frac{1}{1+r^*}\rho^\beta - \tilde{\delta}_{b^{a*}}^q + \frac{1-\varsigma}{b^{a*}}}{\frac{2}{2\sigma-1}\frac{1}{1+r^*}(1-\rho^\beta) + \tilde{\delta}_{b^{a*}}^q + \frac{b^{a^*}\Gamma}{1-2b^{a^*}\Gamma}\left[\frac{2}{2\sigma-1}\frac{1}{1+r^*} + \frac{1-\varsigma}{b^{a*}}\right]}.$$

Around $\Gamma = 0$, the expression multiplying $\frac{b^{a*}\Gamma}{1-2b^{a*}\Gamma}$ in each expression is positive for r^* small and $b^{a*} > 0$ (which is implied by $\beta^* < \beta$). It follows that an increase in Γ amplifies the response of the expected carry trade return and dampens the response of the expected dollar appreciation. In the latter case, this means it reduces the expected dollar depreciation upon a negative $\hat{\epsilon}_t^\beta$ innovation.

Finally, consider the Fama (1984) coefficient. We have that

$$\begin{aligned}
\hat{b}_t^{a*} &= \delta_\beta^{b^{a*}}\hat{\beta}_t + \delta_{b^{a*}}^{b^{a*}}\hat{b}_{t-1}^{a*}, \\
&= \delta_\beta^{b^{a*}}\hat{\beta}_t + \delta_{b^{a*}}^{b^{a*}}\delta_\beta^{b^{a*}}\hat{\beta}_{t-1} + \left(\delta_{b^{a*}}^{b^{a*}}\right)^2\hat{b}_{t-2}^{a*}, \\
&\vdots \\
&= \delta_\beta^{b^{a*}}\sum_{\tau=0}^{\infty}\sum_{s=0}^{\tau}\left(\delta_{b^{a*}}^{b^{a*}}\right)^s\left(\rho^\beta\right)^{\tau-s}\hat{\epsilon}_{t-\tau}^\beta,
\end{aligned}$$

$$= \delta_\beta^{b^{a*}} \sum_{\tau=0}^{\infty} \frac{\left(\rho^\beta\right)^{\tau+1} - \left(\delta_{b^{a*}}^{b^{a*}}\right)^{\tau+1}}{\rho^\beta - \delta_{b^{a*}}^{b^{a*}}} \hat{\epsilon}_{t-\tau}^\beta.$$

Thus, for $x \in \{q, r, r^*\}$,

$$\begin{aligned}\hat{x}_t &= \delta_\beta^x \hat{\beta}_t + \delta_{b^{a*}}^x \hat{b}_{t-1}^{a*}, \\ &= \delta_\beta^x \hat{\epsilon}_t^\beta + \sum_{\tau=0}^{\infty} \left[\delta_\beta^x \left(\rho^\beta\right)^{\tau+1} + \delta_{b^{a*}}^x \delta_\beta^{b^{a*}} \frac{\left(\rho^\beta\right)^{\tau+1} - \left(\delta_{b^{a*}}^{b^{a*}}\right)^{\tau+1}}{\rho^\beta - \delta_{b^{a*}}^{b^{a*}}} \right] \hat{\epsilon}_{t-1-\tau}^\beta.\end{aligned}$$

In the autarkic limit, it follows that

$$\begin{aligned}&\Delta \hat{q}_{t+1} = \delta_\beta^q \hat{\epsilon}_{t+1}^\beta \\ &+ \sum_{\tau=0}^{\infty} \left[\delta_\beta^q \left(\left(\rho^\beta\right)^{\tau+1} - \left(\rho^\beta\right)^{\tau} \right) + \tilde{\delta}_{b^{a*}}^q \tilde{\delta}_\beta^{b^{a*}} \frac{\left(\left(\rho^\beta\right)^{\tau+1} - \left(\delta_{b^{a*}}^{b^{a*}}\right)^{\tau+1} \right) - \left(\left(\rho^\beta\right)^{\tau} - \left(\delta_{b^{a*}}^{b^{a*}}\right)^{\tau} \right)}{\rho^\beta - \delta_{b^{a*}}^{b^{a*}}} \right] \hat{\epsilon}_{t-\tau}^\beta\end{aligned}$$

and

$$\hat{r}_t^* - \hat{r}_t = \sum_{\tau=0}^{\infty} \left(\delta_\beta^{r^*} - \delta_\beta^r\right) \left(\rho^\beta\right)^\tau \hat{\epsilon}_{t-\tau}^\beta.$$

Then

$$\begin{aligned}&Cov(\Delta \hat{q}_{t+1}, \hat{r}_t^* - \hat{r}_t) / \left(\sigma^\beta\right)^2 \\ &= \sum_{\tau=0}^{\infty} \left[\delta_\beta^q \left(\left(\rho^\beta\right)^{\tau+1} - \left(\rho^\beta\right)^{\tau} \right) + \tilde{\delta}_{b^{a*}}^q \tilde{\delta}_\beta^{b^{a*}} \frac{\left(\left(\rho^\beta\right)^{\tau+1} - \left(\delta_{b^{a*}}^{b^{a*}}\right)^{\tau+1} \right) - \left(\left(\rho^\beta\right)^{\tau} - \left(\delta_{b^{a*}}^{b^{a*}}\right)^{\tau} \right)}{\rho^\beta - \delta_{b^{a*}}^{b^{a*}}} \right] \times \\ &\qquad \left[\left(\delta_\beta^{r^*} - \delta_\beta^r\right) \left(\rho^\beta\right)^\tau \right], \\ &= \left(\delta_\beta^{r^*} - \delta_\beta^r\right) \left[-\delta_\beta^q \frac{1}{1+\rho^\beta} + \tilde{\delta}_{b^{a*}}^q \tilde{\delta}_\beta^{b^{a*}} \frac{1}{1+\rho^\beta} \frac{1}{1 - \delta_{b^{a*}}^{b^{a*}} \rho^\beta} \right].\end{aligned}$$

And

$$\begin{aligned}Var(\hat{r}_t^* - \hat{r}_t) / \left(\sigma^\beta\right)^2 &= \left(\delta_\beta^{r^*} - \delta_\beta^r\right)^2 \sum_{\tau=0}^{\infty} \left(\rho^\beta\right)^{2\tau}, \\ &= \left(\delta_\beta^{r^*} - \delta_\beta^r\right)^2 \frac{1}{1 - \left(\rho^\beta\right)^2}.\end{aligned}$$

Hence,

$$\frac{Cov(\Delta\hat{q}_{t+1}, \hat{r}_t^* - \hat{r}_t)}{Var(\hat{r}_t^* - \hat{r}_t)} = -\frac{\delta_\beta^q}{\delta_\beta^{r^*} - \delta_\beta^r}(1-\rho^\beta) + \frac{\tilde{\delta}_{b^{a*}}^q \tilde{\delta}_\beta^{b^{a*}}}{\delta_\beta^{r^*} - \delta_\beta^r} \frac{1-\rho^\beta}{1-\delta_{b^{a*}}^{b^{a*}}\rho^\beta}.$$

Now substituting in for δ_β^q, $\tilde{\delta}_\beta^{b^{a*}}$, and $\delta_\beta^{r^*} - \delta_\beta^r = 1$ yields the Fama (1984) coefficient

$$\frac{Cov(\Delta\hat{q}_{t+1}, \hat{r}_t^* - \hat{r}_t)}{Var(\hat{r}_t^* - \hat{r}_t)} = \frac{\left(1 + \frac{b^{a*}\Gamma}{1-2b^{a*}\Gamma}\right)\left[\frac{2}{2\sigma-1}\frac{1}{1+r^*}(1-\rho^\beta) + \tilde{\delta}_{b^{a*}}^q \frac{1-\rho^\beta}{1-\delta_{b^{a*}}^{b^{a*}}\rho^\beta}\right]}{\frac{2}{2\sigma-1}\frac{1}{1+r^*}(1-\rho^\beta) + \tilde{\delta}_{b^{a*}}^q + \frac{b^{a*}\Gamma}{1-2b^{a*}\Gamma}\left[\frac{2}{2\sigma-1}\frac{1}{1+r^*} + \frac{1-\varsigma}{b^{a*}}\right]}.$$

The derivative of this expression with respect to Γ evaluated at $\Gamma = 0$ is proportional to

$$\begin{aligned}
&\frac{d\tilde{\delta}_{b^{a*}}^q}{d\Gamma}|_{\Gamma=0} + \frac{2}{2\sigma-1}\frac{r^*}{1+r^*}\frac{\rho^\beta}{1-\rho^\beta}\frac{d\delta_{b^{a*}}^{b^{a*}}}{d\Gamma}|_{\Gamma=0} + b^{a*}\left(\frac{2}{2\sigma-1}\frac{1}{1+r^*}(1-\rho^\beta) + \frac{2}{2\sigma-1}\frac{r^*}{1+r^*}\right) \\
&\quad - \left(\frac{d\tilde{\delta}_{b^{a*}}^q}{d\Gamma}|_{\Gamma=0} + b^{a*}\left[\frac{2}{2\sigma-1}\frac{1}{1+r^*} + \frac{1-\varsigma}{b^{a*}}\right]\right) \\
&\quad = b^{a*}\left[-\frac{1}{1-\rho^\beta}\left(-\frac{2}{2\sigma-1}\frac{r^*}{1+r^*} + \frac{1-\varsigma}{b^{a*}}\right) - \frac{2}{2\sigma-1}\frac{1}{1+r^*}\rho^\beta\right],
\end{aligned}$$

which is negative for $b^{a*} > 0$ and r^* small. Thus, the Fama (1984) coefficient falls as Γ rises. □

C Additional empirical analysis

We now provide additional empirical results accompanying those in section 4.

C.1 Alternative approaches to inference

Since both exchange rates and many of the other variables in our analysis are highly persistent, conventional inference can substantially understate the degree of uncertainty in our estimates, especially in small samples. Our preferred method of inference in this context is to use Newey and West (1987) standard errors with truncation parameter equal to sample size and fixed-b critical values, following Kiefer and Vogelsang (2002a,b). Here we compare this approach to alternatives. For brevity we report results for three of our main specifications: the univariate comovement of the exchange

rate with the 10-year yield differential (Table 7) and with relative consumption (Table 8), and the bivariate comovement with the 10-year yield differential and excess bond premium (Table 9). Similar conclusions are obtained for our other specifications.

We consider four versions of inference using Newey and West (1987) standard errors. The first sets the truncation parameter S equal to $0.75N^{1/3}$ where N is the sample size (which evaluates to 4 in our context), a widely followed rule of thumb since Andrews (1991), and standard normal critical values. We next increase the truncation parameter to $1.3N^{1/2}$ (which evaluates to 14 in our context), an updated rule of thumb proposed by Lazarus, Lewis, Stock, and Watson (2018), and then to the sample size itself, following Kiefer and Vogelsang (2002a,b). Rather than using standard normal critical values, we also use fixed-b critical values (where $b = S/N$) using the formula provided in Kiefer and Vogelsang (2005). As is evident from Tables 7-9, the confidence intervals for our estimated coefficients widen as we increase the truncation parameter and use fixed-b critical values.

We next consider three versions of inference using the moving block bootstrap. For each specification, we create 5,000 pseudo-samples by using the estimated coefficients and drawing blocks with replacement from the estimated residuals. For each pseudo-sample, we re-estimate the specification, and we use the distribution of estimates as our confidence intervals. We consider block sizes of 1; 4-5; or 23-29, in the latter two cases choosing a value which evenly divides the sample size. We find that increasing the block size increases the width of the confidence intervals, consistent with the simulation results of Kiefer and Vogelsang (2005) when variables are highly persistent.

We finally consider a VAR-based bootstrap, following Engel (2016). We estimate a two-lag VAR in the log real exchange rate, three-month yield differential, 10-year yield differential, log relative consumption, log U.S. net trade, and excess bond premium over our maintained sample period, 1991 Q2 – 2020 Q1.[47] Given the estimated coefficients, we then create 5,000 pseudo-samples by drawing from the VAR residuals with replacement.[48] For each pseudo-sample, we estimate the comovements of interest, and we again use the distribution of estimates as our confidence intervals.

We settle on Newey and West (1987) standard errors with truncation parameter equal to sample size and fixed-b critical values as our baseline form of inference in

[47]The results which follow are not meaningfully affected using three lags.

[48]We initialize the state variables of the VAR to their average values in our sample, and we draw pseudo-samples which are 1,000 quarters longer than our observed sample so we can discard the first 1,000 quarters as a burn-in period.

	Changes			
	1 qtr	4 qtrs	12 qtrs	Levels
10y (G10 - USD) yield	-2.77	-4.21	-5.87	-8.48
NW: $S = 0.75N^{1/3}$, N	[-4.85,-0.69]	[-7.37,-1.04]	[-9.18,-2.56]	[-10.51,-6.44]
NW: $S = 1.3N^{1/2}$, N	[-4.78,-0.76]	[-6.75,-1.66]	[-8.64,-3.11]	[-11.06,-5.90]
NW: $S = 1.3N^{1/2}$, b	[-5.11,-0.43]	[-7.18,-1.23]	[-9.14,-2.60]	[-11.51,-5.45]
NW: $S = N$, b	[-6.42,0.87]	[-6.52,-1.89]	[-9.28,-2.46]	[-13.35,-3.61]
Bootstrap, $\ell = 1$	[-4.71,-0.82]	[-6.50,-1.91]	[-8.25,-3.52]	[-10.21,-6.74]
Bootstrap, $\ell = 4, 5$	[-4.61,-0.87]	[-7.64,-0.87]	[-9.92,-1.72]	[-11.48,-5.35]
Bootstrap, $\ell = 23 - 29$	[-4.65,-0.79]	[-8.40,-0.16]	[-12.53,0.36]	[-13.33,-3.18]
Bootstrap, VAR	[-4.98,-0.88]	[-7.90,-0.16]	[-14.89,-0.78]	[-18.28,-1.88]
N	115	112	104	116
Adj R^2	0.04	0.07	0.13	0.36
Bootstrap, $\ell = 1$	[-0.00,0.12]	[0.01,0.16]	[0.05,0.25]	[0.25,0.47]
Bootstrap, $\ell = 4, 5$	[-0.00,0.12]	[-0.00,0.22]	[0.00,0.35]	[0.17,0.57]
Bootstrap, $\ell = 23 - 29$	[-0.00,0.12]	[-0.01,0.25]	[-0.01,0.48]	[0.06,0.64]
Bootstrap, VAR	[-0.00,0.13]	[-0.01,0.22]	[-0.00,0.47]	[0.01,0.60]

Table 7: comovements with log real exchange rate between U.S. and G10

Notes: columns marked "Changes" regress 1-, 4-, or 12-quarter change in log real exchange rate on 1-, 4-, or 12-quarter change in given variable. Column marked "Levels" regresses log real exchange rate on given variable. Rows in brackets report 90% confidence intervals using different methods. NW refers to Newey and West (1987) standard errors with truncation parameter S; N refers to critical values from standard normal distribution, while b refers to critical values from asymptotics with fixed $b = S/N$ as reported by Kiefer and Vogelsang (2002a,b, 2005). Bootstrap uses moving blocks with length ℓ or VAR described in text.

the paper. It is more conservative than Newey and West (1987) standard errors with lower truncation parameters or standard normal critical values, and is comparable to the bootstrap methods with large block size or a VAR to address persistence.

We also note that using any of these approaches, a higher 10-year yield differential or relative G10/U.S. consumption is significantly associated with a weaker dollar. The bootstrap specifications imply there is substantial uncertainty about the univariate R^2 of these variables, but in the bivariate specification with the 10-year yield differential and excess bond premium, the lower bound of the R^2 reaches nearly 30%.

	Changes			
	1 qtr	4 qtrs	12 qtrs	Levels
Log G10/U.S. real cons.	-1.75	-3.02	-3.91	-2.59
NW: $S = 0.75N^{1/3}$, N	[-2.80,-0.70]	[-4.29,-1.75]	[-5.38,-2.45]	[-3.49,-1.68]
NW: $S = 1.3N^{1/2}$, N	[-2.71,-0.79]	[-4.02,-2.02]	[-5.80,-2.03]	[-3.85,-1.32]
NW: $S = 1.3N^{1/2}$, b	[-2.86,-0.63]	[-4.19,-1.85]	[-6.14,-1.69]	[-4.07,-1.10]
NW: $S = N$, b	[-2.70,-0.80]	[-4.23,-1.80]	[-6.25,-1.58]	[-4.61,-0.56]
Bootstrap, $\ell = 1$	[-3.12,-0.35]	[-4.19,-1.80]	[-4.94,-2.88]	[-3.20,-1.97]
Bootstrap, $\ell = 4, 5$	[-3.10,-0.39]	[-4.81,-1.20]	[-5.75,-2.06]	[-3.76,-1.40]
Bootstrap, $\ell = 23 - 29$	[-3.06,-0.35]	[-4.80,-1.08]	[-6.45,-1.57]	[-4.65,-0.59]
Bootstrap, VAR	[-3.16,-0.41]	[-5.55,-0.76]	[-8.29,-0.93]	[-8.75,-1.64]
N	115	112	104	116
Adj R^2	0.03	0.13	0.27	0.29
Bootstrap, $\ell = 1$	[-0.01,0.11]	[0.04,0.23]	[0.16,0.40]	[0.18,0.40]
Bootstrap, $\ell = 4, 5$	[-0.01,0.11]	[0.02,0.30]	[0.09,0.52]	[0.11,0.50]
Bootstrap, $\ell = 23 - 29$	[-0.01,0.10]	[0.01,0.26]	[0.05,0.56]	[0.01,0.64]
Bootstrap, VAR	[-0.01,0.10]	[-0.00,0.29]	[0.00,0.57]	[0.03,0.70]

Table 8: comovements with log real exchange rate between U.S. and G10

Notes: columns marked "Changes" regress 1-, 4-, or 12-quarter change in log real exchange rate on 1-, 4-, or 12-quarter change in given variable. Column marked "Levels" regresses log real exchange rate on given variable. Rows in brackets report 90% confidence intervals using different methods. NW refers to Newey and West (1987) standard errors with truncation parameter S; N refers to critical values from standard normal distribution, while b refers to critical values from asymptotics with fixed $b = S/N$ as reported by Kiefer and Vogelsang (2002a,b, 2005). Bootstrap uses moving blocks with length ℓ or VAR described in text.

C.2 Exchange rates and financial conditions

We next provide additional results on the comovement between the real exchange rate and proxies for risk or convenience yields. The main text reported results using the excess bond premium of Gilchrist and Zakrajsek (2012), while here we report results using the VIX, the global factor in risky asset prices of Miranda-Agrippino and Rey (2020), and the three-month Treasury basis from Du et al. (2018).[49] Tables 10-12 provide univariate and bivariate comovements with the dollar/G10 exchange rate.

The results echo those for the excess bond premium in the main text. A higher

[49]We find similar results using convenience yields from Jiang et al. (2021) or Engel and Wu (2023).

	Changes			
	1 qtr	4 qtrs	12 qtrs	Levels
10y (G10 - USD) yield	-5.41	-7.28	-9.14	-9.36
NW: $S = 0.75N^{1/3}$, N	[-7.24,-3.58]	[-10.74,-3.82]	[-12.34,-5.95]	[-11.46,-7.27]
NW: $S = 1.3N^{1/2}$, N	[-6.94,-3.88]	[-10.46,-4.10]	[-12.14,-6.14]	[-12.39,-6.34]
NW: $S = 1.3N^{1/2}$, b	[-7.19,-3.63]	[-11.00,-3.56]	[-12.69,-5.60]	[-12.92,-5.81]
NW: $S = N$, b	[-6.80,-4.02]	[-10.67,-3.89]	[-13.80,-4.49]	[-16.11,-2.62]
Bootstrap, $\ell = 1$	[-7.40,-3.42]	[-9.45,-5.20]	[-11.04,-7.27]	[-10.88,-7.80]
Bootstrap, $\ell = 4, 5$	[-7.32,-3.45]	[-10.30,-4.31]	[-12.31,-6.00]	[-12.15,-6.59]
Bootstrap, $\ell = 23 - 29$	[-7.35,-3.31]	[-10.97,-3.63]	[-14.22,-4.29]	[-14.05,-4.58]
Bootstrap, VAR	[-7.59,-3.75]	[-10.87,-4.44]	[-16.72,-4.61]	[-19.31,-6.11]
EBP	4.20	5.42	8.28	7.09
NW: $S = 4$, N	[2.96,5.44]	[3.90,6.94]	[5.41,11.15]	[2.37,11.81]
NW: $S = 1.3N^{1/2}$, N	[2.99,5.41]	[4.21,6.63]	[4.81,11.75]	[1.66,12.52]
NW: $S = 1.3N^{1/2}$, b	[2.79,5.61]	[4.01,6.84]	[4.18,12.38]	[0.71,13.47]
NW: $S = N$, b	[2.42,5.98]	[4.35,6.50]	[4.22,12.35]	[1.95,12.23]
Bootstrap, $\ell = 1$	[2.74,5.65]	[4.01,6.84]	[6.74,9.79]	[5.24,9.00]
Bootstrap, $\ell = 4, 5$	[2.82,5.62]	[3.41,7.34]	[5.66,10.91]	[4.02,10.14]
Bootstrap, $\ell = 23 - 29$	[2.71,5.67]	[3.15,7.67]	[4.78,11.86]	[3.45,11.20]
Bootstrap, VAR	[2.85,5.53]	[3.88,7.38]	[4.21,12.05]	[5.32,13.56]
N	115	112	104	116
Adj R^2	0.19	0.32	0.50	0.51
Bootstrap, $\ell = 1$	[0.10,0.32]	[0.22,0.44]	[0.41,0.61]	[0.42,0.61]
Bootstrap, $\ell = 4, 5$	[0.10,0.32]	[0.19,0.49]	[0.36,0.67]	[0.37,0.69]
Bootstrap, $\ell = 23 - 29$	[0.09,0.31]	[0.16,0.50]	[0.29,0.73]	[0.27,0.77]
Bootstrap, VAR	[0.10,0.33]	[0.21,0.54]	[0.22,0.68]	[0.28,0.77]

Table 9: additional comovements using proxy for risk

Notes: columns marked "Changes" regress 1-, 4-, or 12-quarter change in log real exchange rate on 1-, 4-, or 12-quarter change in given variable. Column marked "Levels" regresses log real exchange rate on given variable. EBP refers to excess bond premium from Gilchrist and Zakrajsek (2012) and kept updated by Favara et al. (2016). Rows in brackets report 90% confidence intervals using different methods. NW refers to Newey and West (1987) standard errors with truncation parameter S; N refers to critical values from standard normal distribution, while b refers to critical values from asymptotics with fixed $b = S/N$ as reported by Kiefer and Vogelsang (2002a,b, 2005). Bootstrap uses moving blocks with length ℓ or VAR described in text.

	Changes			
	1 qtr	4 qtrs	12 qtrs	Levels
VIX	0.14	0.26	0.30	0.34
	[-0.02,0.29]	[0.16,0.37]	[-0.17,0.78]	[-0.43,1.11]
N	115	112	104	116
Adj R^2	0.06	0.08	0.05	0.05
3m (G10 - USD) yield	-2.13	-1.83	-1.16	-3.28
	[-4.12,-0.14]	[-4.92,1.27]	[-3.81,1.50]	[-7.53,0.97]
VIX	0.14	0.30	0.36	0.34
	[-0.00,0.27]	[0.16,0.44]	[-0.05,0.76]	[-0.16,0.85]
N	115	112	104	116
Adj R^2	0.11	0.13	0.07	0.25
10y (G10 - USD) yield	-4.87	-6.28	-7.86	-8.69
	[-6.03,-3.71]	[-9.99,-2.57]	[-14.72,-1.00]	[-16.43,-0.95]
VIX	0.21	0.38	0.49	0.39
	[0.09,0.33]	[0.21,0.55]	[0.17,0.81]	[0.05,0.72]
N	115	112	104	116
Adj R^2	0.17	0.22	0.27	0.42

Table 10: additional comovements using proxy for risk

Notes: columns marked "Changes" regress 1-, 4-, or 12-quarter change in log real exchange rate on 1-, 4-, or 12-quarter change in given variable. Column marked "Levels" regresses log real exchange rate on given variable. Rows in brackets report 90% confidence intervals using Newey and West (1987) standard errors with truncation parameter equal to sample size and fixed-b critical values, following Kiefer and Vogelsang (2002a,b).

	Changes			
	1 qtr	4 qtrs	12 qtrs	Levels
Global factor	-3.73	-3.66	-3.67	-3.58
	[-5.35,-2.11]	[-5.42,-1.91]	[-6.98,-0.36]	[-8.96,1.81]
N	111	108	100	112
Adj R^2	0.19	0.18	0.11	0.07
3m (G10 - USD) yield	-2.35	-1.99	-2.76	-4.06
	[-3.81,-0.88]	[-3.97,-0.01]	[-5.01,-0.51]	[-5.18,-2.93]
Global factor	-3.81	-3.98	-6.18	-5.77
	[-4.81,-2.81]	[-4.99,-2.97]	[-10.01,-2.35]	[-7.87,-3.67]
N	111	108	100	112
Adj R^2	0.25	0.24	0.22	0.36
10y (G10 - USD) yield	-6.67	-8.06	-11.53	-9.77
	[-8.24,-5.10]	[-10.73,-5.38]	[-14.12,-8.93]	[-13.47,-6.06]
Global factor	-5.45	-5.15	-7.60	-5.76
	[-6.26,-4.63]	[-6.24,-4.06]	[-11.76,-3.44]	[-9.49,-2.04]
N	111	108	100	112
Adj R^2	0.40	0.41	0.50	0.54

Table 11: additional comovements using proxy for risk

Notes: columns marked "Changes" regress 1-, 4-, or 12-quarter change in log real exchange rate on 1-, 4-, or 12-quarter change in given variable. Column marked "Levels" regresses log real exchange rate on given variable. Global factor in risky asset prices is from Miranda-Agrippino and Rey (2020). Rows in brackets report 90% confidence intervals using Newey and West (1987) standard errors with truncation parameter equal to sample size and fixed-b critical values, following Kiefer and Vogelsang (2002a,b).

	Changes			
	1 qtr	4 qtrs	12 qtrs	Levels
3m Treasury basis	0.92	0.17	-0.20	-0.51
	[-0.24,2.08]	[-1.37,1.72]	[-5.14,4.74]	[-9.51,8.49]
N	115	112	104	116
Adj R^2	0.00	-0.01	-0.01	-0.01
3m (G10 - USD) yield	-2.09	-1.40	-0.68	-3.44
	[-4.43,0.25]	[-4.09,1.28]	[-2.55,1.20]	[-6.60,-0.28]
3m Treasury basis	0.35	0.23	-0.70	-3.46
	[-0.79,1.49]	[-2.09,2.55]	[-5.65,4.25]	[-5.19,-1.73]
N	115	112	104	116
Adj R^2	0.04	0.02	-0.01	0.20
10y (G10 - USD) yield	-2.67	-4.28	-5.87	-8.56
	[-6.62,1.29]	[-6.53,-2.03]	[-9.31,-2.44]	[-12.89,-4.23]
3m Treasury basis	0.71	0.75	-0.15	-2.08
	[-0.55,1.97]	[-0.80,2.31]	[-6.09,5.80]	[-5.07,0.90]
N	115	112	104	116
Adj R^2	0.03	0.06	0.12	0.35

Table 12: additional comovements using proxy for risk

Notes: columns marked "Changes" regress 1-, 4-, or 12-quarter change in log real exchange rate on 1-, 4-, or 12-quarter change in given variable. Column marked "Levels" regresses log real exchange rate on given variable. 3m Treasury basis is from Du et al. (2018), updated through 2020 using data shared with us by Wenxin Du. Rows in brackets report 90% confidence intervals using Newey and West (1987) standard errors with truncation parameter equal to sample size and fixed-b critical values, following Kiefer and Vogelsang (2002a,b).

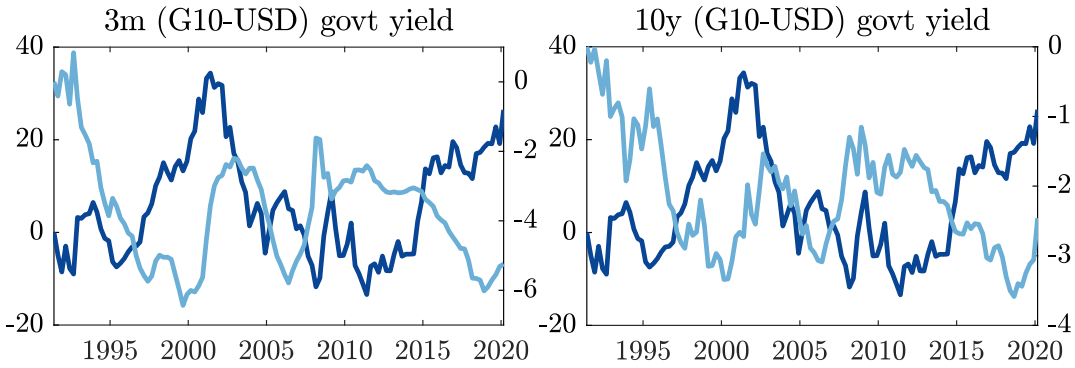

Figure 7: comovements with log real exchange rate and government yield differentials

Notes: dark blue line in each panel is log real exchange rate, plotted on left axis; light blue line in each panel is series in panel title, plotted on right axis. All series plotted in *pp*. All series are normalized to zero in 1991 Q2. All yields are annualized.

VIX or lower level of global risky asset prices is associated with a stronger dollar (interestingly, this is not consistently the case for a higher Treasury basis). In changes, these variables account for a comparable or higher share of the variation than yield differentials; in levels, they account for much less of the variation in the exchange rate. And again, in bivariate specifications, the explanatory power together is greater than the sum of their parts, and we can account for as much as 50% of the exchange rate variation both in changes and levels.

C.3 Exchange rates and government bond yield differentials

We next replace the private sector interest rate differentials — constructed from Libor rates and interest rate swaps — with government bond yield differentials. The first two panels of Table 13 report the analogs of the first two panels of Table 1 in the main text using government bond yields. Figure 7 depicts the comovements of the dollar/G10 real exchange rate with these government bond yield differentials. The third and fourth panels of Table 13 report the analogs of the latter two panels of Table 2 using government bond yield differentials and the excess bond premium.

The results echo those with private sector interest rate differentials. The dollar is strong when G10 government bond yields are low versus U.S. government bond yields. This is not the case in the early 2000s, 2008, and 2020. So when we also condition on a proxy for risk such as the excess bond premium, the comovement of the exchange rate with government bond yield differentials strengthens, and the share of variation

	Changes			
	1 qtr	4 qtrs	12 qtrs	Levels
3m (G10 - USD) yield	-1.40	-1.49	-0.63	-3.52
	[-3.86,1.05]	[-3.69,0.71]	[-2.77,1.51]	[-7.02,-0.02]
N	115	112	104	116
Adj R^2	0.01	0.03	-0.00	0.18
10y (G10 - USD) yield	-2.00	-2.98	-4.89	-7.55
	[-6.45,2.46]	[-5.39,-0.58]	[-9.22,-0.56]	[-10.37,-4.72]
N	115	112	104	116
Adj R^2	0.01	0.03	0.08	0.25
3m (G10 - USD) yield	-1.71	-2.26	-2.14	-4.29
	[-4.43,1.01]	[-5.01,0.48]	[-4.34,0.07]	[-7.78,-0.81]
EBP	2.60	4.37	7.26	7.39
	[0.12,5.07]	[3.53,5.22]	[2.14,12.39]	[0.87,13.91]
N	115	112	104	116
Adj R^2	0.08	0.20	0.27	0.34
10y (G10 - USD) yield	-4.73	-6.68	-9.46	-8.83
	[-6.21,-3.25]	[-10.37,-3.00]	[-14.64,-4.28]	[-12.71,-4.95]
EBP	4.02	5.50	8.76	7.43
	[2.26,5.79]	[4.32,6.68]	[4.41,13.11]	[1.47,13.40]
N	115	112	104	116
Adj R^2	0.15	0.27	0.47	0.42

Table 13: comovements with log real exchange rate and government yield differentials

Notes: columns marked "Changes" regress 1-, 4-, or 12-quarter change in log real exchange rate on 1-, 4-, or 12-quarter change in given variable. Column marked "Levels" regresses log real exchange rate on given variable. EBP refers to excess bond premium from Gilchrist and Zakrajsek (2012) and kept updated by Favara et al. (2016). Rows in brackets report 90% confidence intervals using Newey and West (1987) standard errors with truncation parameter equal to sample size and fixed-b critical values, following Kiefer and Vogelsang (2002a,b).

in the exchange rate we can explain rises.

C.4 Bilateral exchange rates and interest rate differentials

We now study the comovement between bilateral real exchange rates and interest rate differentials for each of the G10 countries versus the U.S. Table 14 reports these comovements focusing on the levels specifications for brevity, and Figures 8 and 9 visually depict them.

For all currencies except the Japanese yen, a lower foreign yield than the dollar yield is associated with a stronger real dollar versus that currency. Hence, the comovement which we document between the broad dollar/G10 exchange rate and yield differential in the main text is robust across currencies. The distinct comovement with the yen reflects the fact that over our sample period, Japanese yields have tended to rise relative to U.S. yields (since Japan hit the zero lower bound early in the sample while U.S. yields tended toward zero), and yet Japan has experienced a trend real depreciation versus the U.S. We note that around these trends, low Japanese yields versus U.S. yields have also been associated with a relatively strong dollar, as depicted in Figure 9.

Interestingly, the share of variation in the bilateral exchange rates accounted for by yield differentials differs substantially across countries. The 10-year yield differential, for instance, accounts for only 2% of the variation in the real exchange rate between the U.S. and Canada, but 37% of the variation in the real exchange rate between the U.S. and Sweden. There is substantial uncertainty about these R^2 values in population given the persistence of the variables in question. Nonetheless, exploring these differences across currencies would be an interesting direction for future work, related to the discussion in section 6.

C.5 Alternative base currencies

In this subsection we replace the U.S. with three alternative base currencies and countries: the pound and the U.K., the euro and Euro Area, and the yen and Japan. Tables 15-17 report the analogs to Table 1 for these base currencies and countries, and Figures 10-12 depict the analogs to Figure 1.

These results indicate that the comovements which we document in the main text are not U.S.-specific: when we use the pound as an alternative base currency, we

	3m	10y		3m	10y
AUD	-5.33	-11.45	GBP	-3.99	-7.19
	[-8.70,-1.97]	[-19.60,-3.30]		[-8.75,0.77]	[-16.33,1.94]
N	115	113	N	116	113
Adj R^2	0.22	0.33	Adj R^2	0.37	0.33
CAD	-3.02	-2.99	JPY	1.96	3.56
	[-6.49,0.44]	[-8.35,2.37]		[-1.27,5.20]	[-4.49,11.60]
N	114	113	N	111	105
Adj R^2	0.07	0.02	Adj R^2	0.04	0.04
CHF	-2.83	-9.79	NOK	-1.77	-7.43
	[-7.96,2.29]	[-13.09,-6.49]		[-10.74,7.20]	[-23.38,8.53]
N	105	104	N	82	83
Adj R^2	0.10	0.23	Adj R^2	0.03	0.14
DKK	-2.97	-7.60	NZD	-2.68	-8.53
	[-8.44,2.50]	[-10.77,-4.43]		[-7.24,1.88]	[-21.46,4.39]
N	88	89	N	95	95
Adj R^2	0.10	0.28	Adj R^2	0.04	0.10
EUR	-3.71	-7.52	SEK	-4.24	-7.74
	[-8.86,1.45]	[-14.38,-0.67]		[-9.61,1.13]	[-15.25,-0.24]
N	84	79	N	88	98
Adj R^2	0.14	0.16	Adj R^2	0.23	0.37

Table 14: comovements of log real exchange rate and yield differential

Notes: columns regress log real exchange rate on 3m yield differential (first column) or 10y yield differential (second column) for each currency versus USD. Regressions use Newey and West (1987) standard errors with truncation parameter equal to sample size and fixed-b critical values, following Kiefer and Vogelsang (2002a,b).

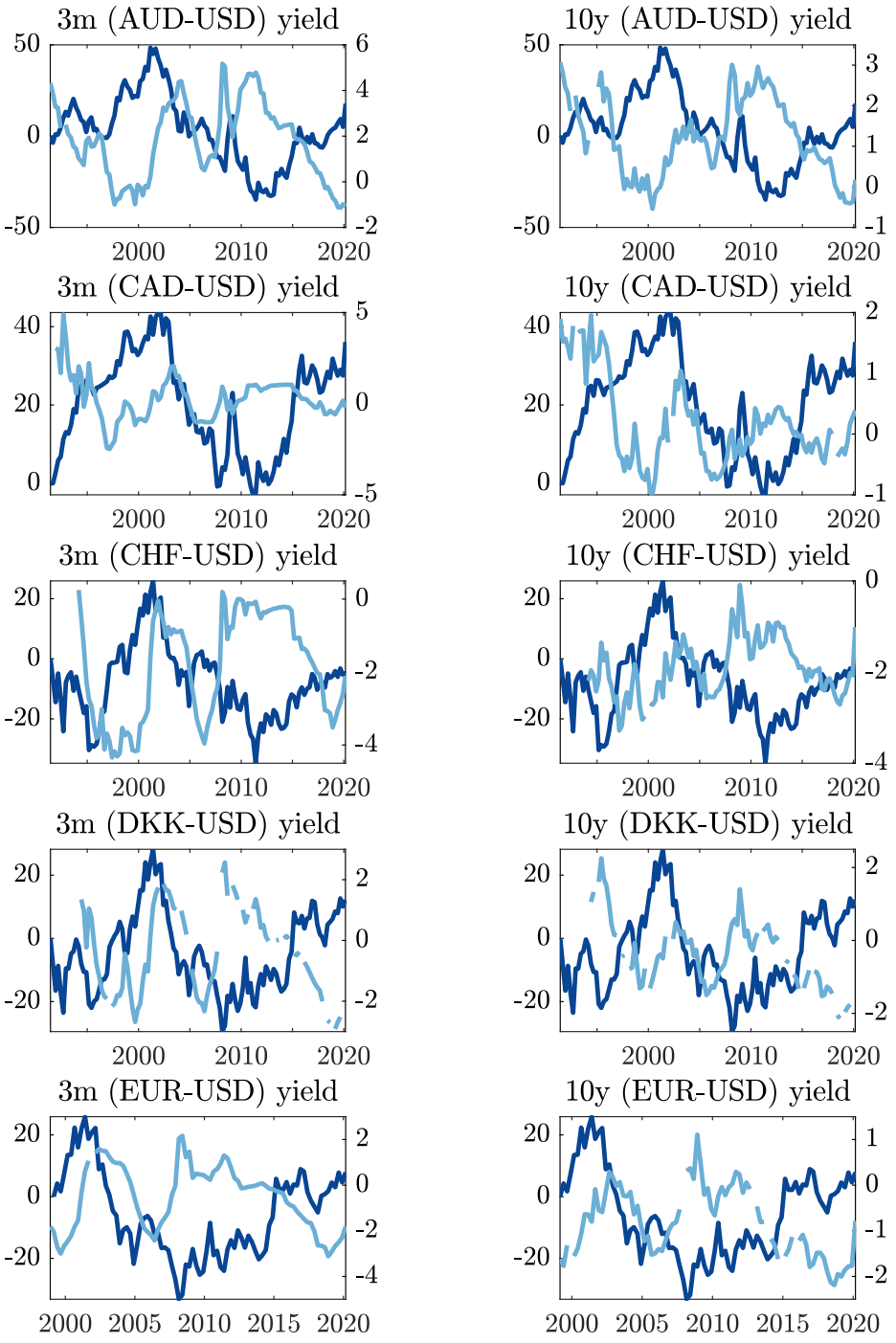

Figure 8: comovements with log real exchange rate and yield differential

Notes: dark blue line in each panel is log real exchange rate, plotted on left axis; light blue line in each panel is series in panel title, plotted on right axis. All series plotted in *pp*. Real exchange rate normalized to zero in 1991 Q2 except for euro, which is normalized to zero in 1999 Q1. All yields are annualized.

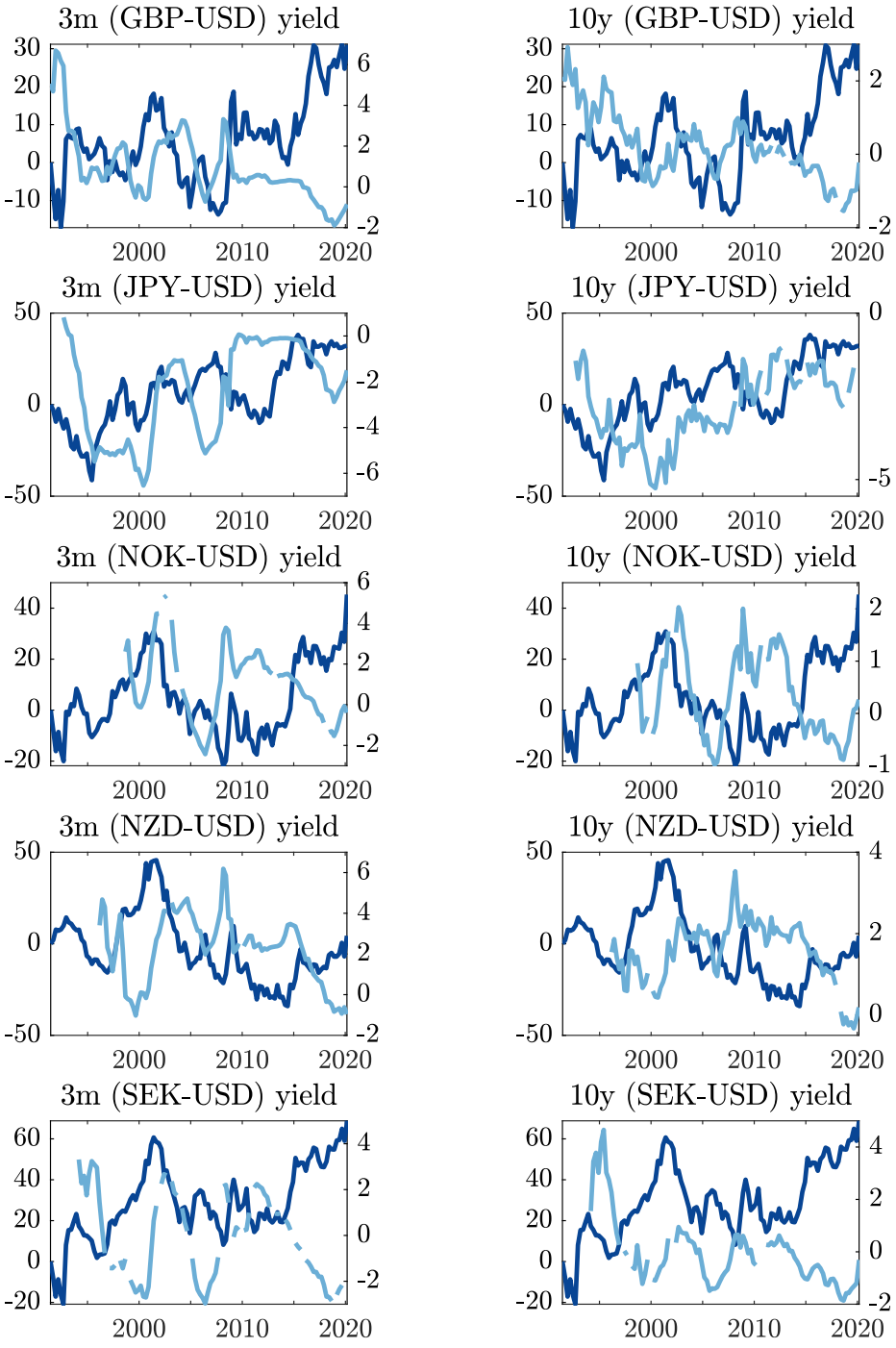

Figure 9: comovements with log real exchange rate and yield differential

Notes: dark blue line in each panel is log real exchange rate, plotted on left axis; light blue line in each panel is series in panel title, plotted on right axis. All series plotted in *pp*. Real exchange rate normalized to zero in 1991 Q2. All yields are annualized.

	Changes			
	1 qtr	4 qtrs	12 qtrs	Levels
3m (G10 - GBP) yield	-3.81	-3.98	-5.27	-6.60
	[-6.02,-1.60]	[-5.51,-2.46]	[-8.65,-1.89]	[-10.90,-2.31]
N	115	112	104	116
Adj R^2	0.23	0.27	0.36	0.56
10y (G10 - GBP) yield	-3.94	-7.09	-5.62	-9.14
	[-8.14,0.25]	[-18.25,4.07]	[-24.37,13.13]	[-25.65,7.38]
N	106	101	94	110
Adj R^2	0.06	0.09	0.04	0.20
Log G10/U.K. real cons.	-0.75	-1.38	-2.38	-2.46
	[-2.00,0.50]	[-3.53,0.78]	[-3.44,-1.32]	[-3.55,-1.37]
N	100	97	89	101
Adj R^2	0.02	0.08	0.40	0.52
Log U.K. net trade	-0.05	-0.09	-1.25	-0.69
	[-0.18,0.08]	[-0.61,0.42]	[-2.41,-0.09]	[-1.54,0.15]
N	115	112	104	116
Adj R^2	-0.01	-0.01	0.16	0.05

Table 15: comovements with log real exchange rate between U.K. and G10

Notes: columns marked "Changes" regress 1-, 4-, or 12-quarter change in log real exchange rate on 1-, 4-, or 12-quarter change in given variable. Column marked "Levels" regresses log real exchange rate on given variable. Regressions use Newey and West (1987) standard errors with truncation parameter equal to sample size and fixed-b critical values, following Kiefer and Vogelsang (2002a,b).

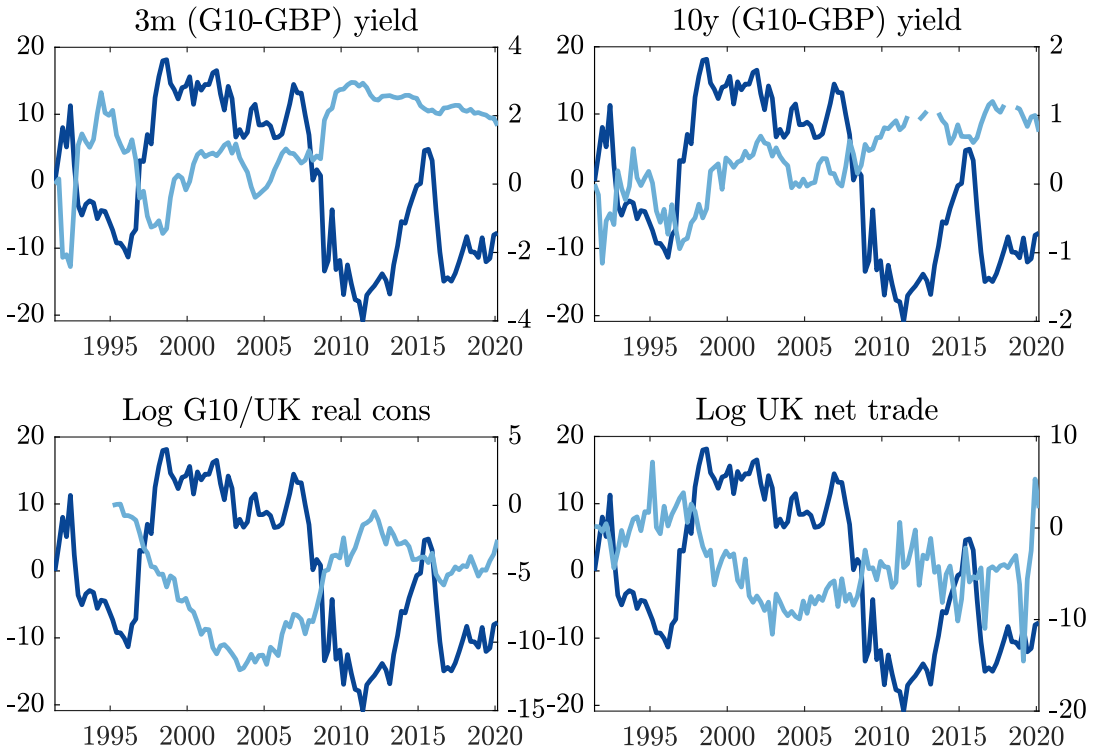

Figure 10: comovements with log real exchange rate between U.K. and G10

Notes: dark blue line in each panel is log real exchange rate, plotted on left axis; light blue line in each panel is series in panel title, plotted on right axis. All series plotted in *pp*. All series except log U.K. net trade are normalized to zero in first quarter. All yields are annualized.

	Changes			
	1 qtr	4 qtrs	12 qtrs	Levels
3m (G10 - EUR) yield	-3.19	-3.36	-3.83	-1.15
	[-6.69,0.31]	[-8.88,2.16]	[-11.03,3.37]	[-9.83,7.53]
N	81	77	70	83
Adj R^2	0.03	0.06	0.06	-0.00
10y (G10 - EUR) yield	-6.55	-4.80	-4.71	-1.10
	[-8.27,-4.83]	[-12.35,2.74]	[-19.94,10.52]	[-18.54,16.34]
N	66	64	53	73
Adj R^2	0.16	0.05	0.02	-0.01
Log G10/EA real cons.	0.20	0.09	-0.05	0.10
	[-1.63,2.03]	[-1.60,1.79]	[-2.08,1.98]	[-0.67,0.88]
N	84	81	73	85
Adj R^2	-0.01	-0.01	-0.01	-0.00
Log EA net trade	-0.12	0.07	-0.30	-0.35
	[-0.43,0.19]	[-0.49,0.64]	[-1.24,0.63]	[-1.57,0.86]
N	84	81	73	85
Adj R^2	-0.01	-0.01	-0.00	0.02

Table 16: comovements with log real exchange rate between Euro area (EA) and G10

Notes: columns marked "Changes" regress 1-, 4-, or 12-quarter change in log real exchange rate on 1-, 4-, or 12-quarter change in given variable. Column marked "Levels" regresses log real exchange rate on given variable. Regressions use Newey and West (1987) standard errors with truncation parameter equal to sample size and fixed-b critical values, following Kiefer and Vogelsang (2002a,b).

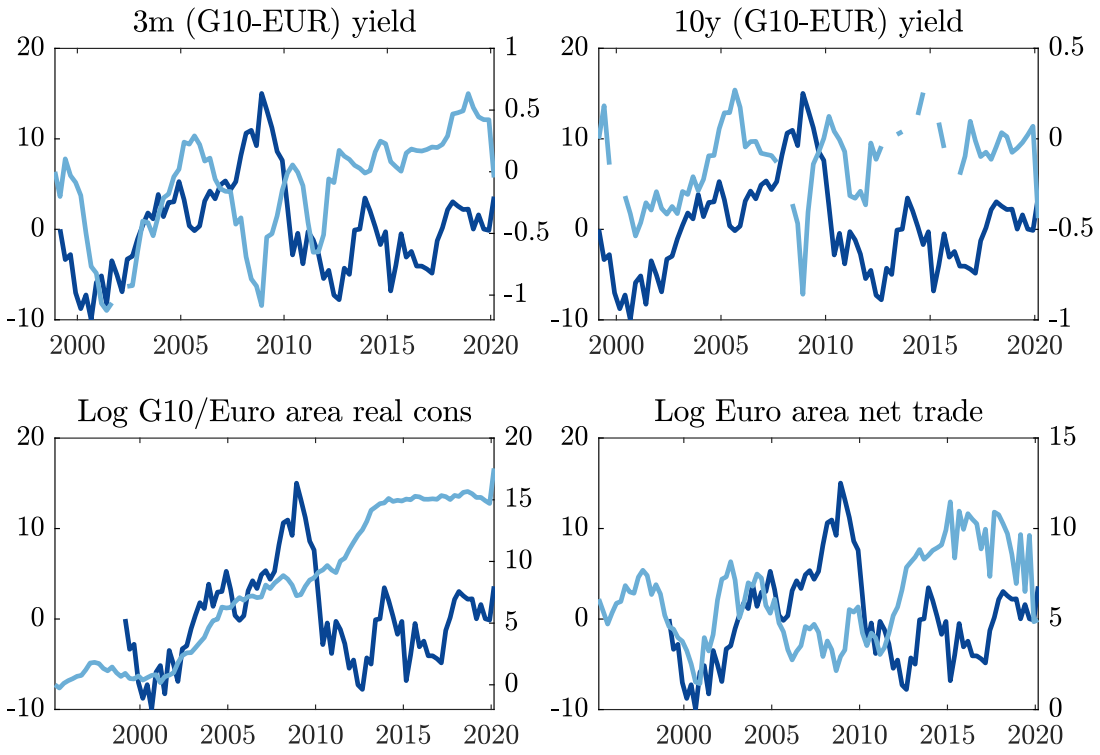

Figure 11: comovements with log real exchange rate between Euro area and G10

Notes: dark blue line in each panel is log real exchange rate, plotted on left axis; light blue line in each panel is series in panel title, plotted on right axis. All series plotted in *pp*. All series except log Euro area net trade are normalized to zero in first quarter. All yields are annualized.

	Changes			
	1 qtr	4 qtrs	12 qtrs	Levels
3m (G10 - JPY) yield	-4.02	-1.45	-2.66	6.54
	[-9.19,1.15]	[-8.63,5.74]	[-10.95,5.64]	[1.95,11.13]
N	110	107	99	111
Adj R^2	0.06	0.01	0.03	0.33
10y (G10 - JPY) yield	-4.05	-0.43	5.60	11.52
	[-11.75,3.65]	[-11.90,11.03]	[-0.08,11.28]	[8.62,14.42]
N	93	87	79	99
Adj R^2	0.06	-0.01	0.07	0.40
Log G10/Japan real cons.	0.35	1.36	1.17	-1.99
	[-2.02,2.73]	[-0.15,2.88]	[-1.21,3.54]	[-2.43,-1.55]
N	104	101	93	105
Adj R^2	-0.01	0.03	0.02	0.56
Log Japan net trade	0.00	0.05	0.35	1.08
	[-0.52,0.53]	[-0.53,0.62]	[-0.02,0.73]	[0.28,1.88]
N	104	101	93	105
Adj R^2	-0.01	-0.01	0.03	0.35

Table 17: comovements with log real exchange rate between Japan and G10

Notes: columns marked "Changes" regress 1-, 4-, or 12-quarter change in log real exchange rate on 1-, 4-, or 12-quarter change in given variable. Column marked "Levels" regresses log real exchange rate on given variable. Regressions use Newey and West (1987) standard errors with truncation parameter equal to sample size and fixed-b critical values, following Kiefer and Vogelsang (2002a,b).

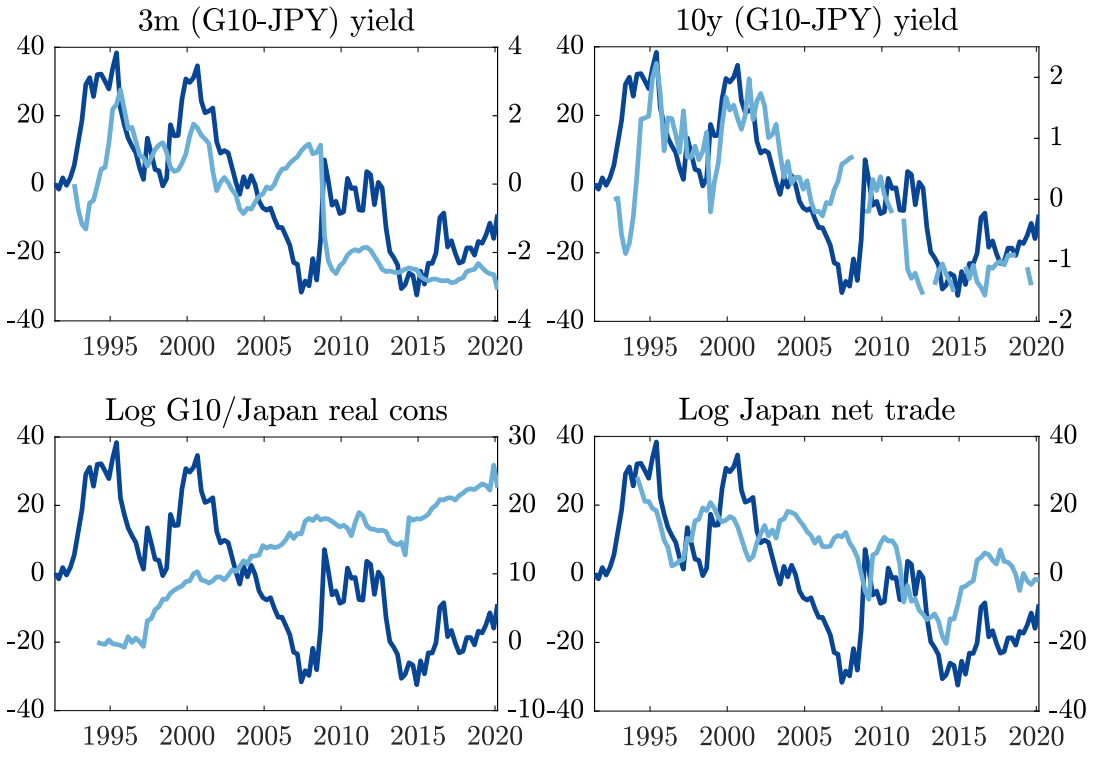

Figure 12: comovements with log real exchange rate between Japan and G10

Notes: dark blue line in each panel is log real exchange rate, plotted on left axis; light blue line in each panel is series in panel title, plotted on right axis. All series plotted in *pp*. All series except log Japan net trade are normalized to zero in first quarter. All yields are annualized.

obtain very similar results. Low G10 interest rates (which now includes the U.S. and excludes the U.K.) relative to U.K. interest rates and low G10 consumption per capita relative to its U.K. counterpart are associated with a stronger pound in real terms versus the G10, both in changes and in levels. In levels, the yield differentials account for 20-56% of the variation, and relative consumption per capita accounts for 52% of the variation, in the real exchange rate.

At the same time, these results are not as sharp for the Euro area and Japan. In the case of the Euro area, this reflects the shorter sample period of available data, which puts more weight on the early 2000s period in which a strengthening euro was accompanied by falling Euro area yields and consumption relative to the rest of the G10. While the early 2000s also featured a breakdown of the typical comovement between the dollar/G10 exchange rate and yield differentials as documented in the main text, these dynamics may also reflect particularities of the early years of the euro. In the case of Japan, the comovements with yield differentials (in levels) were strikingly positive prior to the mid-2000s. Related to the discussion in section 6 and the prior subsection, understanding these comovements for Japan seems a valuable direction for future work.

C.6 Low frequency comovements

We next study the comovements between the low frequency components of the exchange rate and other variables, following Müller and Watson (2018). An advantage of their approach is that it is robust to nonstationarity.

Their methodology works as follows. We project the series depicted in Figure 1 onto cosine functions with periodicities above a particular cutoff. For instance, Figure 13 plots these projections for the log real exchange rate and 10-year yield differential given two cutoffs, 6 years and 12 years. The comovements between these projections capture the long run covariability between these series.[50] Müller and Watson (2018) provide an algorithm to conduct Bayesian inference on the regression and correlation coefficients between these series using a wide prior distribution on their degree of cointegration. We use their algorithm without modification.

Table 18 summarizes regressions of the low frequency component of the log real exchange rate on the low frequency components of other variables. It demonstrates

[50]We say "long run" because these periodicities exceed the typical U.S. business cycle, which has averaged 75 months between 1945-2020 (NBER (n.d.)).

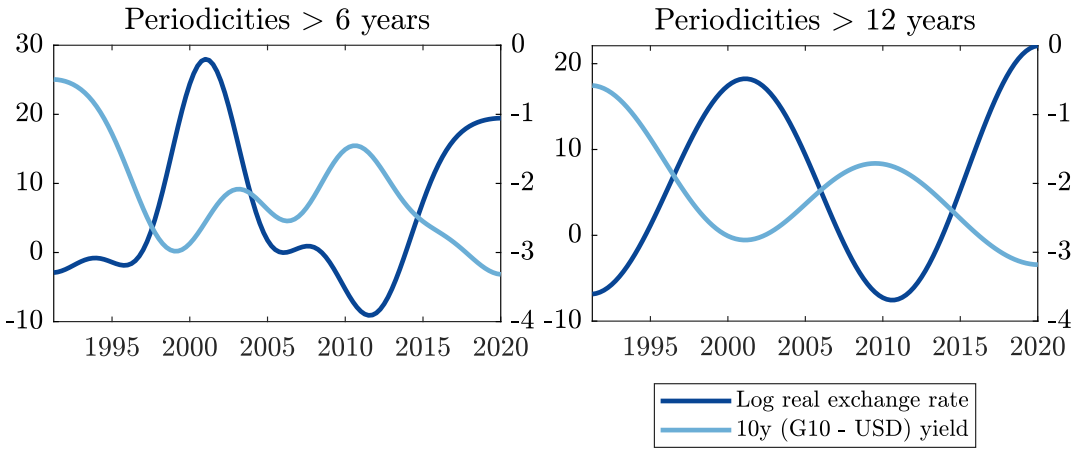

Figure 13: low frequency log real exchange rate and 10-year yield differential

Notes: panels depict projections of each series on cosine functions with periodicities above 6 years (left) or 12 years (right) using Müller and Watson (2018) algorithm. We add a scalar to each projection so that the in-sample mean equals that of the series depicted in Figure 1.

that the results from Table 1 in the main text are robust to this approach focused on low frequencies. The dollar has been strong when G10 yields have been low relative to U.S. yields, and when G10 consumption has been low relative to U.S. consumption. The 90% posterior credible sets exclude zero except for the 3-month yield differential with the 6-year periodicity cutoff, and for relative consumption with the 12-year periodicity cutoff. The share of exchange rate variation explained by these variables ranges between 18-28% for the 6-year periodicity cutoff, and higher values for the 12-year periodicity cutoff, reaching 58% for the 10-year yield differential. The 90% posterior credible sets for these values are wide, however, echoing the results we obtain using the bootstrap earlier in this appendix. There is little evidence of long run covariability between the exchange rate and log U.S. net trade.[51]

The last panel of Table 18 notes that this analysis, while focused on the low frequency components of these series, remains highly relevant to understand most exchange rate variation. It reports that 85% (70%) of the unconditional variation in the log real exchange rate is captured by the projection on periodicities above 6 (12) years. This underscores existing results in the literature that most of the variation in the exchange rate is at low frequencies (e.g., Rabanal and Rubio-Ramirez (2015)).

[51] As discussed in the main text, this may simply reflect delayed adjustment of trade to the exchange rate. Indeed, visually, the low frequency component of the exchange rate appears to lead the low frequency component of U.S. net trade by a few years.

	Periodicities > 6 years	Periodicities > 12 years
3m (G10 - USD) yield	-3.49	-8.00
	[-8.26,1.17]	[-13.45,-2.58]
N	116	116
Adj R^2	0.18	0.58
	[-0.01,0.56]	[0.01,0.94]
10y (G10 - USD) yield	-8.86	-12.73
	[-17.13,-0.53]	[-22.63,-2.61]
N	116	116
Adj R^2	0.27	0.52
	[-0.01,0.66]	[0.00,0.93]
Log G10/U.S. real cons.	-3.16	-3.31
	[-6.12,-0.33]	[-7.83,1.18]
N	116	116
Adj R^2	0.28	0.33
	[-0.01,0.66]	[-0.01,0.84]
Log U.S. net trade	-0.31	-0.28
	[-1.15,0.49]	[-1.55,0.95]
N	116	116
Adj R^2	0.11	0.16
	[-0.01,0.40]	[-0.01,0.60]
Memo:		
% Var(log real exchange rate)	85%	70%

Table 18: low frequency comovements with log real exchange rate

Notes: each panel regresses low frequency component of log real exchange rate on low frequency component of given variable, using Müller and Watson (2018) methodology. Rows in brackets report 90% posterior credible sets. Last panel reports share of variation of log real exchange rate accounted for by its projection on cosine functions with periodicities above 6 or 12 years.

C.7 Out-of-sample explanatory power

We finally study the ability of yield differentials, measures of risk or convenience yields, and relative quantities to explain the exchange rate out of sample. We follow the methodology of Meese and Rogoff (1983) and the large subsequent literature surveyed in Rossi (2013).

In particular, we estimate the contemporaneous specification in changes

$$\log q_{t+h} - \log q_t = \alpha + \beta \left(x_{t+h} - x_t \right) + \epsilon_{t+h},$$

where x_t is a candidate explanatory variable. We estimate this specification over a rolling 60 quarter sample, beginning with 1991 Q2 through 2005 Q1. With coefficients α_{t-1} and β_{t-1} estimated using forecasts through $t - 1 + h$, we use these estimated coefficients and the realized change in the explanatory variable $x_{t+h} - x_t$ to form the forecast $\log q_{t+h} - \log q_t$ and then compute the error versus the data. We repeat this process for all dates t between 2005 Q2 and the last date we make a forecast in our sample, 2020 Q1 less h, and we summarize the out-of-sample fit with the root mean squared error (RMSE) of forecast errors. We compare this to the RMSE obtained using the random walk, which simply predicts that

$$\log q_{t+h} - \log q_t = \epsilon_{t+h}.$$

We conduct inference on the mean squared errors by constructing the Clark and West (2006) test statistic.

Over the past 30 years, we can do better than a random walk in explaining the exchange rate out of sample. Table 19 reports the results from the data at three forecast horizons, $h = \{1, 4, 12\}$ quarters, using yield differentials, proxies for risk or convenience yields, and these together, along with relative consumption and log U.S. net trade. The three-month yield differential, excess bond premium, VIX, and global factor in risky asset prices significantly outperform the random walk at short horizons, though their individual performances deteriorate as the horizon extends. The 10-year yield differential and relative consumption outperform the random walk at four- and 12-quarters ahead, though the differences in the first case are not statistically significant at conventional levels. Combining the 10-year yield differential with the excess bond premium, VIX, or global factor in risky asset prices significantly outperforms the random walk at all horizons. The only variables which cannot beat a random walk at any horizon are net trade and the Treasury basis, consistent with their weak in-sample comovements evident from Tables 1 and 12.

	$h = 1$		$h = 4$		$h = 12$	
	RMSE	CW	RMSE	CW	RMSE	CW
Random walk	3.9		8.0		11.7	
3m (G10 - USD yield)	3.7	2.57***	8.0	0.39	12.9	−1.23
10y (G10 - USD yield)	3.9	−0.18	7.9	1.10	11.6	0.84
EBP	3.7	1.51*	8.1	0.87	12.6	0.54
and 3m (G10 - USD yield)	3.5	2.66***	7.6	1.45*	11.4	2.67***
and 10y (G10 - USD yield)	3.4	2.96***	6.9	2.06**	8.8	2.29**
VIX	3.7	1.55*	7.7	1.82**	13.2	−0.52
and 3m (G10 - USD yield)	3.5	2.24**	7.2	2.59***	12.2	0.62
and 10y (G10 - USD yield)	3.4	2.56***	6.7	3.32***	9.0	1.85**
Global factor	3.1	3.68***	6.7	2.48***	13.2	−0.82
and 3m (G10 - USD yield)	2.8	4.02***	5.8	2.78***	11.6	1.25
and 10y (G10 - USD yield)	2.4	4.30***	4.8	3.01***	8.9	1.50*
3m Treasury basis	4.3	−1.44	8.4	−0.85	13.4	−1.36
and 3m (G10 - USD yield)	4.1	−0.64	8.1	0.37	13.1	−1.37
and 10y (G10 - USD yield)	4.3	−1.24	8.0	0.84	11.6	0.62
Log G10/U.S. real cons. p.c.	3.9	0.81	7.3	1.96**	10.3	2.14**
Log U.S. net trade	4.0	−2.09	8.4	−1.16	13.6	−0.73

Table 19: out-of-sample explanatory power for log real exchange rate

Notes: each row reports root mean squared error (RMSE) and Clark and West (2006) test statistic from specification estimated in changes over rolling 60 quarter sample beginning with 1991 Q2 – 2005 Q1, and forecasting through 2020 Q1. EBP refers to excess bond premium from Gilchrist and Zakrajsek (2012) and kept updated by Favara et al. (2016), global factor in risky asset prices is from Miranda-Agrippino and Rey (2020), and 3m Treasury basis is from Du et al. (2018), updated through 2020 using data shared with us by Wenxin Du. *, **, and *** denote statistical significance at 10%, 5%, and 1% one-sided levels, respectively.

D Additional quantitative analysis

We now provide additional quantitative results accompanying those in section 5.

D.1 Additional untargeted moments in data and model

We first compare additional untargeted moments in the data and model.

Table 20 summarizes untargeted volatilities and autocorrelations of three-month

yields, 10-year yields, and consumption per capita. Recall that we used the stochastic properties of demand shocks to target the volatility and autocorrelation of the 10-year yield differential. While the second panel indicates that the model generates 10-year yields in levels and changes broadly consistent with the data, the first panel indicates that the model implies more volatile three-month yields in levels and changes than in the data. This reflects that three-month yields are smoother than 10-year yields in the data, likely a result of interest rate smoothing by central banks. Since our model does not feature such smoothing, we overstate the volatility of three-month yields; since exchange rates are forward-looking, we do not anticipate such smoothing would have much effect on the model-implied exchange rate.

The last panel indicates that one shortcoming of the model is that it generates excessive volatility in consumption growth relative to the data. This is because relative consumption across countries is too volatile at high frequencies, as reflected in a counterfactually negative correlation of consumption growth between countries in the first row of Table 21. As described in the main text, this reflects the strong contemporaneous response of trade flows to shocks in the model (even with pricing to market). We expect that generalizing the model to account for dynamic trade as in Alessandria and Choi (2007) and Drozd and Nosal (2012) would be one way of delaying this adjustment and bringing these moments closer in line with the data.

The other correlations of consumption and output reported in Table 21 are more comparable between data and model.

D.2 Additional impulse responses

In the main text we presented the model's impulse responses to a demand shock. Figures 14 and 15 depict the impulse responses to supply and intermediation shocks.

A one standard deviation decrease in the U.S. endowment causes a dollar appreciation, decline in the Foreign interest rate relative to the U.S. interest rate, increase in Foreign consumption relative to U.S. consumption, temporary increase in U.S. net trade, and temporary decline in the expected excess return on Foreign bonds less dollar bonds. These results are consistent with Proposition 1. Notably, the response of the exchange rate is an order of magnitude smaller than to discount factor shocks in Figure 3. This reflects that, given the stochastic process for output per capita in the data, endowment shocks induce changes in real interest rates which are both

		σ		ρ_{-1}	
	Variable	Data	Model	Data	Model
$r^{(1)}$	U.S. interest rate	2.19%	2.57%	0.97	0.93
$r^{(1)*}$	Foreign interest rate	2.22%	2.55%	0.98	0.93
$r^{(1)*} - r^{(1)}$	interest rate spread	1.58%	1.50%	0.96	0.89
$\Delta r^{(1)}$	Δ U.S. interest rate	0.51%	0.85%	0.27	-0.02
$\Delta r^{(1)*}$	Δ Foreign interest rate	0.40%	0.83%	0.28	-0.02
$\Delta r^{(1)*} - \Delta r^{(1)}$	Δ interest rate spread	0.43%	0.63%	0.18	-0.05
$r^{(40)}$	U.S. 10y yield	2.01%	1.66%	0.96	0.93
$r^{(40)*}$	Foreign 10y yield	2.40%	1.66%	0.99	0.93
$\Delta r^{(40)}$	Δ U.S. 10y yield	0.53%	0.53%	-0.00	-0.01
$\Delta r^{(40)*}$	Δ Foreign 10y yield	0.39%	0.53%	0.18	-0.02
$\Delta r^{(40)*} - r^{(40)}$	Δ 10y yield spread	0.30%	0.26%	-0.06	-0.02
$\Delta \log c$	Δ U.S. consumption	0.50%	0.81%	0.36	-0.04
$\Delta \log c^*$	Δ Foreign consumption	0.44%	0.70%	0.39	-0.04

Table 20: untargeted volatilities and autocorrelations in data and model

Notes: model moments are averages over 1,000 simulations of 116 quarters each using a 1,000 quarter burn-in period.

	Data	Model
$\rho(\Delta \log c, \Delta \log c^*)$	0.59	-0.54
$\rho(\Delta \log c, \Delta \log y)$	0.87	0.79
$\rho(\Delta \log c^*, \Delta \log y^*)$	0.74	0.76
$\rho(\Delta \log y, \Delta \log y^*)$	0.31	0.03

Table 21: untargeted comovements in data and model

Notes: model moments are averages over 1,000 simulations of 116 quarters each using a 1,000 quarter burn-in period.

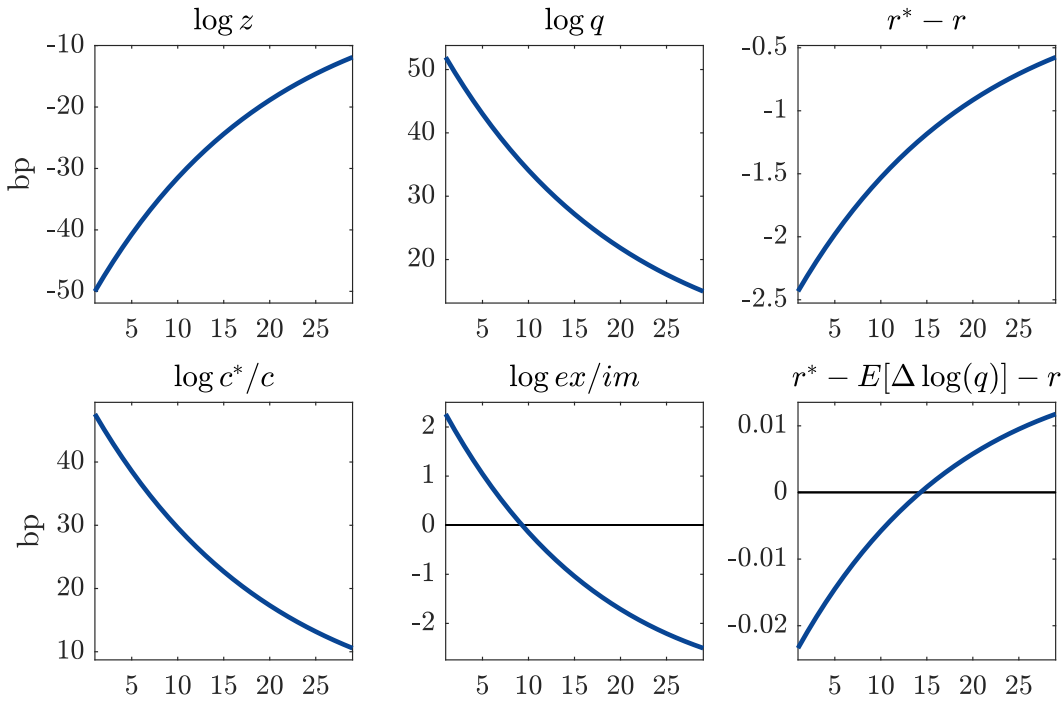

Figure 14: impulse responses to supply shock

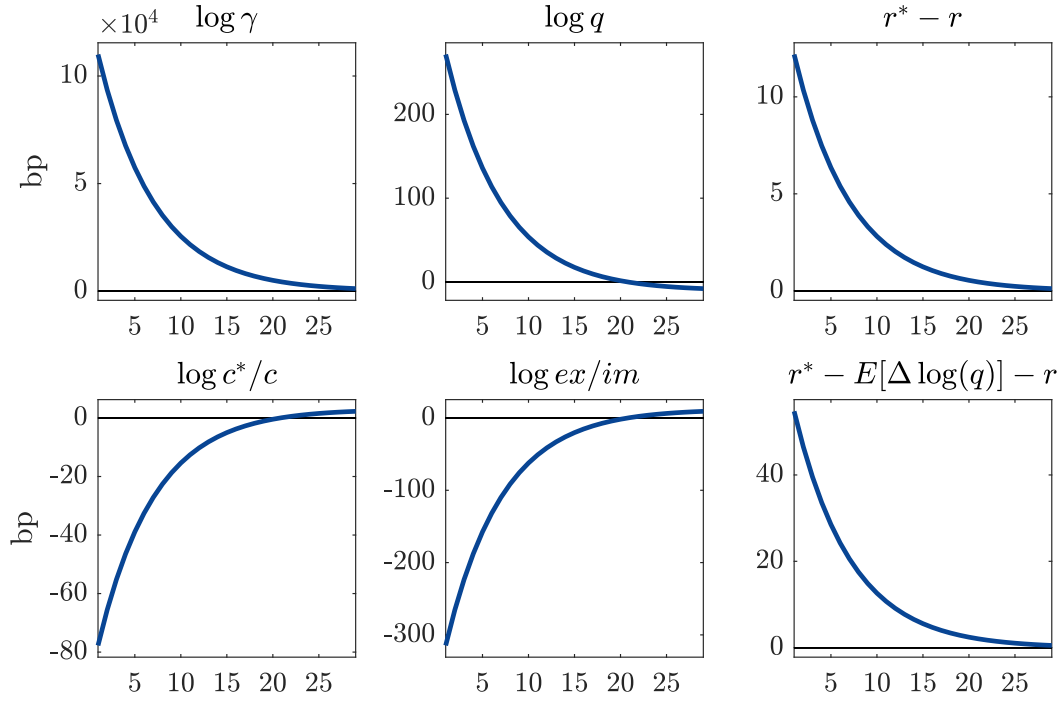

Figure 15: impulse responses to currency intermediation shock

smaller and less persistent than discount factor shocks, the latter disciplined by the stochastic properties of bond yields themselves.

A one standard deviation increase in arbitrageur risk aversion causes a dollar appreciation, increase in the Foreign interest rate relative to the U.S. interest rate, decline in Foreign consumption relative to U.S. consumption, decline in U.S. net trade, and increase in the expected excess return on Foreign bonds less dollar bonds. These results are again consistent with Proposition 1. The response of the exchange rate is less persistent than in the case of discount factor shocks. This reflects that the excess bond premium, which we use to discipline arbitrageur risk aversion shocks, is less persistent than bond yields, which discipline discount factor shocks.

D.3 Comovements of exchange rate in changes

In the main text we compared the model-implied comovements between the real exchange rate, yield differentials, and quantities to the empirical counterparts, all run in a levels specification. Table 22 compares the model and data in our changes specifications, where the latter estimates are from the first three columns of Table 1.

The model-generated comovements between changes in the exchange rate and changes in interest rate differentials get more negative, and the R^2 rises, as the horizon of changes increases, and as the tenor of the bond increases. These patterns reflect that changes in arbitrageur risk aversion are more transitory than changes in relative demand, so the specifications over longer horizons and using longer tenors increasingly reflect relative demand shocks. Most of the model-implied coefficients, though not all, are within or just outside the empirical confidence intervals, and the model-implied R^2 coefficients are not too much higher than in the data.

The model-generated comovements between changes in the exchange rate and changes in quantities reflect the results from the levels specification discussed in the main text. The model accounts well for the negative comovement between the dollar and relative consumption at all horizons, though it overstates the R^2s. The model-implied negative comovement with U.S. net trade in changes is outside the empirical confidence intervals and the model again substantially overstates the R^2s. Later in this appendix we demonstrate how an extended version of the model featuring trade shocks can make progress in resolving these inconsistencies versus the data.

	1-qtr changes		4-qtr changes		12-qtr changes	
	Data	Model	Data	Model	Data	Model
$\log q$ on $r^{(1)*} - r^{(1)}$						
Coeff	[-4.54,0.19]	0.97	[-4.03,1.22]	0.40	[-2.75,1.46]	-0.71
Adj R^2	0.05	0.02	0.03	0.02	-0.00	0.06
$\log q$ on $r^{(40)*} - r^{(40)}$						
Coeff	[-6.42,0.87]	-6.62	[-6.52,-1.89]	-7.43	[-9.28,-2.46]	-8.55
Adj R^2	0.04	0.18	0.07	0.25	0.13	0.37
$\log q$ on $\log c^* - \log c$						
Coeff	[-2.70,-0.80]	-2.35	[-4.23,-1.80]	-2.31	[-6.25,-1.58]	-2.24
Adj R^2	0.03	0.59	0.13	0.57	0.27	0.55
$\log q$ on $\log ex/im$						
Coeff	[-0.33,0.17]	-0.86	[-0.51,0.30]	-0.86	[-0.75,0.24]	-0.86
Adj R^2	-0.01	0.97	-0.01	0.96	0.02	0.96

Table 22: exchange rate comovements in changes in data and model

Notes: model moments are averages over 1,000 simulations of 116 quarters each using a 1,000 quarter burn-in period.

D.4 Out-of-sample fit

In the main text and prior subsection we compared the model to the data using in-sample comovements. Table 23 instead compares the model's out-of-sample performance to the data. The top panel is taken from Table 19, where we focus on the excess bond premium as a representative proxy for $\log \gamma_t$ consistent with our calibration strategy. The bottom panel replicates the empirical methodology on many model-generated samples of 116 quarters each, averaging the RMSE and Clark and West (2006) statistics across the model simulations.

Out-of-sample forecasting on model-generated data yields generally comparable results as the actual data. The forecast errors in the random walk specification have similar magnitudes as the data at all horizons, validating that the model-generated stochastic properties of the exchange rate are consistent with the data. As in the data, the forecasting ability of the one-quarter yield differential in terms of RMSE relative to the random walk deteriorates with horizon, while it improves with horizon in the case of the 10-year yield differential; arbitrageur risk aversion has significant

	$h = 1$		$h = 4$		$h = 12$	
	RMSE	CW	RMSE	CW	RMSE	CW
Data						
Random walk	3.9		8.0		11.7	
3m (G10 - USD yield)	3.7	2.57^{***}	8.0	0.39	12.9	-1.23
10y (G10 - USD yield)	3.9	-0.18	7.9	1.10	11.6	0.84
EBP	3.7	1.51^{*}	8.1	0.87	12.6	0.54
and 3m (G10 - USD yield)	3.5	2.66^{***}	7.6	1.45^{*}	11.4	2.67^{***}
and 10y (G10 - USD yield)	3.4	2.96^{***}	6.9	2.06^{**}	8.8	2.29^{**}
Log G10/U.S. real cons. p.c.	3.9	0.81	7.3	1.96^{**}	10.3	2.14^{**}
Log U.S. net trade	4.0	-2.09	8.4	-1.16	13.6	-0.73
Model						
Random walk	4.5		8.1		13.0	
$r_t^{(1)*} - r_t^{(1)}$	4.6	-1.10	8.4	-0.27	13.2	0.30
$r_t^{(40)*} - r_t^{(40)}$	3.6	4.82^{***}	7.1	2.35^{***}	11.5	0.97
$\log \gamma_t$	3.3	6.05^{***}	6.3	2.96^{***}	7.2	1.75^{**}
and $r_t^{(1)*} - r_t^{(1)}$	0.5	7.37^{***}	1.0	4.43^{***}	2.1	2.51^{***}
and $r_t^{(40)*} - r_t^{(40)}$	0.4	7.40^{***}	1.0	4.40^{***}	2.3	2.53^{***}
$\log c_t^*/c_t$	2.9	5.62^{***}	4.7	3.76^{***}	6.5	3.09^{***}
$\log ex/im$	0.8	7.23^{***}	1.2	4.41^{***}	1.6	2.97^{***}

Table 23: out-of-sample explanatory power for log real exchange rate

Notes: on data, each row reports root mean squared error (RMSE) and Clark and West (2006) test statistic from specification estimated in differences over rolling 60 quarter sample beginning with 1991 Q2 – 2005 Q1, and forecasting through 2020 Q1. EBP refers to excess bond premium from Gilchrist and Zakrajsek (2012) and kept updated by Favara et al. (2016). On model, each row reports same statistics from same specifications estimated on 1,000 model simulations of 116 quarters each using a 1,000 quarter burn-in period. *, **, and *** denote statistical significance at 10%, 5%, and 1% one-sided levels, respectively.

forecasting power at the one-quarter horizon; the combination of risk aversion with yield differentials can significantly outperform a random walk at all horizons; and relative consumption can beat a random walk at long horizons.

There are also some differences from the data. In particular, the 10-year yield differential can significantly outperform the random walk even at short horizons; arbitrageur risk aversion can significantly outperform the random walk at long horizons;

and the magnitude of the RMSEs is quite small using the combination of risk aversion and yield differentials versus the data. These discrepancies are to be expected if the 10-year yield differential and excess bond premium are noisy measures of the expected path of interest rate differentials and arbitrageurs' risk bearing capacity in practice. Moreover, relative consumption can beat a random walk at short horizons, and net trade can also beat a random walk at all horizons, unlike the data. These are consistent with trade flows (and thus consumption) responding too quickly to relative prices in the model, as previously discussed.

D.5 Spanning regressions

Chernov and Creal (2023) and Chernov et al. (2024) find relatively low R^2 coefficients in regressions projecting exchange rate changes on local currency asset returns, implying that local currency asset returns do not span exchange rates. Here we reproduce their empirical findings and then demonstrate that our model generates comparable R^2 coefficients in such regressions, even though the dominant drivers of the exchange rate are demand shocks which also drive bond yields.

Given a set of bond maturities $\mathcal{T}$, Chernov et al. (2024) report the R^2 from regressions of the form

$$\log q_{t+1} - \log q_t = \alpha + \sum_{\tau \in \mathcal{T}} \left[\beta^{(\tau)} r^{(\tau)}_{t,t+1} + \beta^{(\tau)*} r^{(\tau)*}_{t,t+1} \right] + \epsilon_{t+1}, \tag{27}$$

where

$$\begin{aligned} r^{(\tau)}_{t,t+1} &= \log p^{(\tau-1)}_{t+1} - \log p^{(\tau)}_t, \\ r^{(\tau)*}_{t,t+1} &= \log p^{(\tau-1)*}_{t+1} - \log p^{(\tau)*}_t \end{aligned}$$

denote the dollar and foreign returns on τ-period local currency bonds from t to $t+1$, respectively. That is, they ask whether changes in the exchange rate are spanned by both U.S. and foreign bond returns over that same period. Chernov and Creal (2023) run closely related regressions, and the results which follow also hold when we reproduce their specifications.

The first panel and column of Table 24 estimates specification (27) on our data. We average the R^2 values obtained from bilateral specifications for each G10 currency; while we use Libor rates and quarterly data (as throughout the paper) whereas Cher-

$\mathcal{T}$	Data	Model	Model + τ-specific shocks
$\log q_{t+1} - \log q_t$ on $r^{(\tau)}_{t,t+1}$ and $r^{(\tau)*}_{t,t+1}$ for $\tau \in \mathcal{T}$			
{8}	0.08	0.02	0.02
{20}	0.11	0.10	0.08
{40}	0.11	0.20	0.18
{8,20,40}	0.19	0.90	0.26
{8,12,20,28,40}	0.27	0.99	0.29
$r^{(40)}_{t,t+1}$ on $r^{(\tau)}_{t,t+1}$ for $\tau \in \mathcal{T}$			
{8}	0.63	0.89	0.70
{20}	0.93	0.99	0.92
{8,20}	0.97	1.00	0.92
{8,12,20,28}	1.00	1.00	0.96
$r^{(40)*}_{t,t+1}$ on $r^{(\tau)*}_{t,t+1}$ for $\tau \in \mathcal{T}$			
{8}	0.58	0.89	0.71
{20}	0.90	0.99	0.92
{8,20}	0.95	1.00	0.93
{8,12,20,28}	0.99	1.00	0.96

Table 24: R^2 from spanning regressions in data and model

Notes: columns report R^2 from regression reported in panel title. For data, values in first and third panels are averaged across bilateral specifications for each G10 currency. For model, last column adds shocks to yield curve in each country as described in main text. All statistics averaged over 1,000 model simulations of 116 quarters each using a 1,000 quarter burn-in period.

nov et al. (2024) use government bond yields and monthly data, the R^2 values we obtain are comparable to theirs.[52] Returns on single maturities in the U.S. and abroad explain no more than 11% of the quarterly variation in the exchange rate, and even using five maturities in each country we obtain only 27% spanning.

The second column demonstrates that model-generated data features comparable

[52]Since we only observe bond yields at selected tenors, we approximate returns as follows. Given a T-quarter zero coupon bond with annualized yield $y_t(T)$ at date t, its log price is $\log P(y_t(T), T) = -(T/4)\log(1 + y_t(T))$. Assuming for simplicity that the yield on a $T-1$ quarter bond is the same as a T quarter bond at $t+1$, we can approximate the log return on a T-quarter bond between t and $t+1$ as $\log P(y_{t+1}(T-1), T-1) - \log P(y_t(T), T) \approx \log P(y_{t+1}(T), T) + (1/4)\log(1 + y_{t+1}(T)) - \log P(y_t(T), T)$.

$\mathcal{T}$	Data	Model	Model + τ-specific shocks
$\log q_{t+1} - \log q_t$ on $r^{(\tau)}_{t,t+1}$ and $r^{(\tau)*}_{t,t+1}$ for $\tau \in \mathcal{T}$			
{8}	$1E+02$	$5E+01$	$4E+01$
{20}	$8E+01$	$7E+01$	$5E+01$
{40}	$5E+01$	$7E+01$	$6E+01$
{8,20,40}	$3E+02$	$2E+03$	$1E+02$
{8,12,20,28,40}	$1E+03$	$4E+15$	$1E+02$
$r^{(40)}_{t,t+1}$ on $r^{(\tau)}_{t,t+1}$ for $\tau \in \mathcal{T}$			
{8}	$3E+02$	$3E+02$	$3E+02$
{20}	$2E+02$	$2E+02$	$2E+02$
{8,20}	$3E+02$	$2E+02$	$1E+02$
{8,12,20,28}	$2E+02$	$5E+02$	$1E+02$
$r^{(40)*}_{t,t+1}$ on $r^{(\tau)*}_{t,t+1}$ for $\tau \in \mathcal{T}$			
{8}	$3E+02$	$3E+02$	$3E+02$
{20}	$2E+02$	$2E+02$	$2E+02$
{8,20}	$2E+02$	$2E+02$	$1E+02$
{8,12,20,28}	$2E+02$	$5E+02$	$1E+02$

Table 25: 100 times maximal absolute value of spanning coefficients in data and model

Notes: columns report 100 times maximal absolute value of coefficients on dollar and foreign assets from regression reported in panel title. For data, values in first and third panels are averaged across bilateral specifications for each G10 currency. For model, last column adds shocks to yield curve in each country as described in main text. All statistics averaged over 1,000 model simulations of 116 quarters each using a 1,000 quarter burn-in period.

R^2 values for spanning regressions with a single maturity. This reflects the presence of both demand and intermediation shocks in the model, which are roughly equally important in driving exchange rate variation at short horizons. Demand shocks and intermediation shocks which have the same effect on the exchange rate have contrasting effects on local currency bond returns, implying that these bond returns explain only a limited share of the variation in the exchange rate at short horizons.

As we add more local currency bond returns to the right-hand side of these regressions, the spanning regressions on model-generated data of course feature much higher R^2 values because the model features a finite set of shocks. Importantly, however, the

implied spanning portfolios involve unrealistically large positions. Table 25 reports 100 times the maximal absolute value of regression coefficients in (27), which can be interpreted as the maximal weight in the portfolio of bonds which most closely replicates the exchange rate. Using five maturities in each currency on model-generated data, this maximal portfolio weight is 10^{12} times larger than in the data.

Spanning regressions of long-maturity bond returns on shorter-maturity returns suggest that our model is missing shocks along each country's yield curve. The second and third panels of Table 24 report R^2 values from these regressions. Whereas in the data, variation in two-year bond returns in each country explains around 60% of the variation in 10-year bond returns, in the model the same statistic is nearly 90%.

This motivates the following simple extension of our model. In each country, we add small maturity-specific shocks to the pricing equations for long-term bonds $\{\eta_t^{(\tau)}\}$ and $\{\eta_t^{(\tau)*}\}$, so that the price of a τ-period dollar bond is

$$p_t^{(\tau)} = \mathbb{E}_t \left[\beta_t \left(\frac{c_{t+1}}{c_t} \right)^{-1/\psi} \exp\left(\eta_t^{(\tau)} \right) p_{t+1}^{(\tau-1)} \right],$$

and analogously for Foreign bonds. These shocks may reflect convenience yields that households in each country receive from bonds of different maturities; localized demand shocks in a richer model of the term structure, as in Vayanos and Vila (2021) and Gourinchas et al. (2024); or simply measurement error when mapping the model to the data. To avoid discontinuities in the yield curve (and in keeping with the first two interpretations), we parametrize the shocks across maturities as smooth functions of N underlying structural shocks. In the U.S., we assume

$$\eta_t^{(\tau)} = \sum_{n=1}^{N} f_t^n \exp\left(\frac{-(\tau - 4n)^2}{36} \right),$$

where each shock f_t^n is an *iid* normal innovation, and analogously in Foreign. Each of the N shocks in each country therefore has a bell-shaped effect on all maturities centered around maturity $4n$. We consider $N = 10$ shocks (thus centered around maturities $1, 2, \ldots, 10$ years) and set the standard deviation of each shock to $\sigma^f = \sigma^{f*} = 0.004$. Figure 16 plots the effects of one standard deviation shocks on the yield curve in each country. These shocks are so small and transitory that they leave all of the second moments in bond yields in Table 4 unchanged up to reported precision;

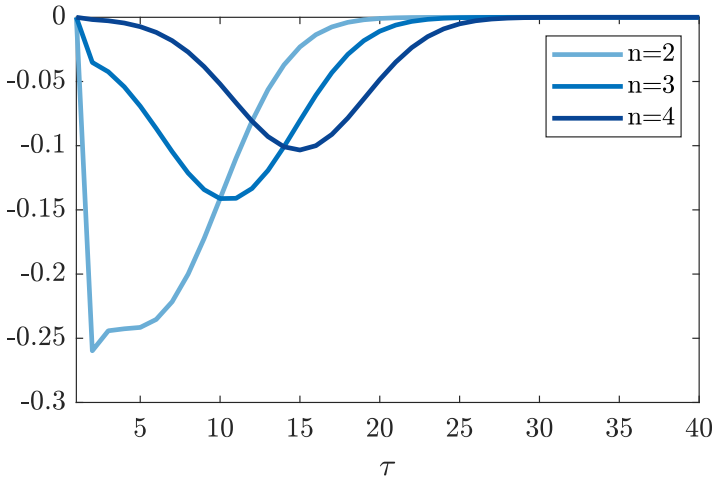

Figure 16: effects of noise shocks $\{f_t^n\}$ along each country's yield curve

Notes: figure depicts effects of one standard deviation shock to $\{f_t^2, f_t^3, f_t^4\}$ on annualized yield curve $-(\tau/4)\log p_t^{(\tau)}$, expressed in *pp*.

since they only affect the pricing of long-term bonds, they also leave the rest of the allocation (including exchange rates) exactly unchanged.

Adding these shocks brings spanning regressions in the model fully in line with the data. We see in the last column of Table 24 that the R^2 values of 10-year bond returns on shorter-maturity bond returns in each country are now more comparable between model and data, and the R^2 values of exchange rates on multiple local currency bond returns falls sharply. The reason is that the small amount of noise in bond returns substantially dampens the portfolio weights in the last column of Table 25, making them comparable to the data. Intuitively, once there exists very small noise in bond returns, one can no longer take massive offsetting positions along the term structure to recover the exchange rate.

D.6 Additional simulation results over 1991-2020

We now present additional simulation results using the shocks recovered from 10-year yields, output per capita, and the excess bond premium series in the data.

Figure 17 depicts relative consumption and U.S. net trade in data and model. The first panel indicates that the model successfully generates the low-frequency movement in relative consumption observed in the data. At the same time, it is more volatile at higher frequencies than the data. The second panel similarly demonstrates that trade

flows are more volatile at higher frequencies than the data, and also demonstrates that for extended periods the model-implied net trade series leads that in the data. These observations are all consistent with trade flows responding too quickly to the exchange rate in the model. As discussed earlier, we expect that accounting for investment, dynamic trade, or trade shocks could close the gap. The next subsection explores a model extension with trade shocks to illustrate these ideas.

Figure 18 compares proxies for risk with the unexplained component of the exchange rate using only demand shocks extracted from 10-year yields. The excess bond premium, VIX, and global factor in risky asset prices especially covary with the unexplained component, demonstrating that they complement demand shocks in accounting for the dollar/G10 exchange rate. This mirrors the incremental explanatory power these proxies have in accounting for the exchange rate in Tables 2, 10, and 11.

D.7 Extension to trade shocks

We next present an extension of our model featuring trade shocks. These shocks mitigate the baseline model's counterfactually tight connection between the exchange rate, relative consumption, and net trade, without changing our conclusion that demand shocks account for most of the variation in the exchange rate.

We modify Foreign's consumption aggregator to be

$$c_t^* = \left(\left(\frac{1}{1+\zeta^*}(1-\alpha_t\varsigma) \right)^{\frac{1}{\sigma}} (c_{Ht}^*)^{\frac{\sigma-1}{\sigma}} + \left(\frac{\zeta^*}{1+\zeta^*} + \frac{1}{1+\zeta^*}\alpha_t\varsigma \right)^{\frac{1}{\sigma}} (c_{Ft}^*)^{\frac{\sigma-1}{\sigma}} \right)^{\frac{\sigma}{\sigma-1}}.$$

Now, α_t is a driving force controlling Foreign's degree of home bias. We assume $\log \alpha_t$ follows an AR(1) process with mean zero, standard deviation of shocks σ^α, and autocorrelation ρ^α. We assume for simplicity that it has a zero correlation with the other shocks in the model, though in a calibration relaxing this assumption we have found it does not change our main findings.

Figure 19 depicts the impulse responses to a negative innovation to α_t which appreciates the dollar. We use the parameter values described in the next paragraph, but present these impulse responses first to motivate the calibration strategy. The key feature of trade shocks is that they imply that the dollar appreciation is accompanied by an increase in U.S. net trade. This contrasts with both demand and intermediation shocks, for which the expenditure switching mechanism means that a dollar

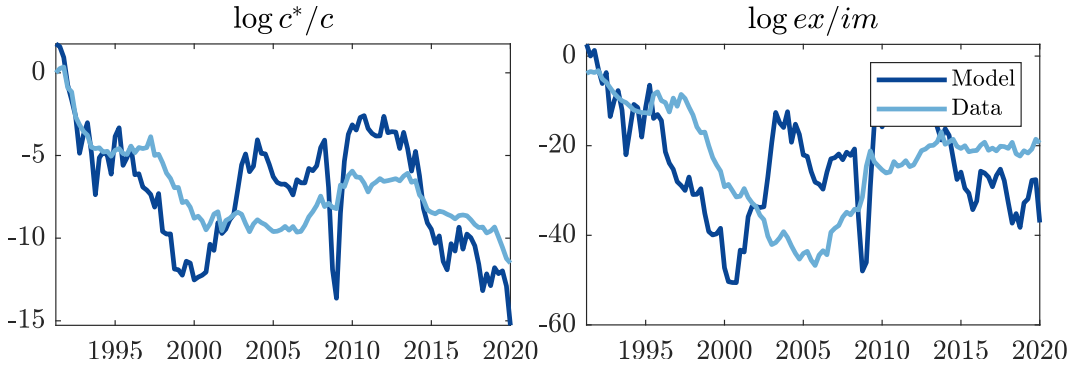

Figure 17: relative consumption and U.S. net trade in data and model

Notes: model-implied exchange rate simulated by inverting $\{\beta_t, \beta_t^*, z_t, z_t^*, \gamma_t\}$ to match 10-year yields and output per capita in U.S. and G10, as well as excess bond premium of Gilchrist and Zakrajsek (2012). All series plotted in *pp*. Constant is added to model-generated series to match same average value as data series.

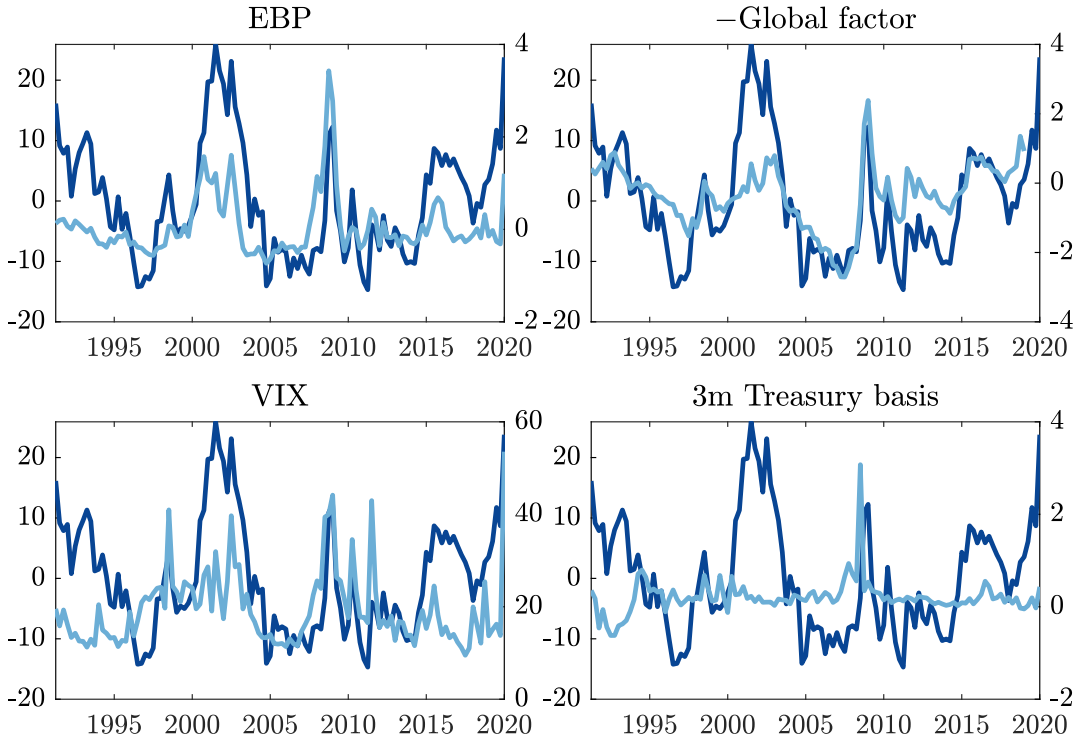

Figure 18: unexplained exchange rate with only demand shocks and proxies for risk

Notes: dark blue line in each panel is data less model with only $\{\epsilon^{\beta}, \epsilon^{\beta^*}\}$ shocks extracted from 10-year yields, plotted on left axis; light blue line in each panel is series in panel title, plotted on right axis. EBP refers to excess bond premium from Gilchrist and Zakrajsek (2012) and kept updated by Favara et al. (2016). Global factor refers to global factor in risky asset prices from Miranda-Agrippino and Rey (2020). Treasury basis is from Du et al. (2018), updated through 2020 using data shared with us by Wenxin Du. All series plotted in *pp*.

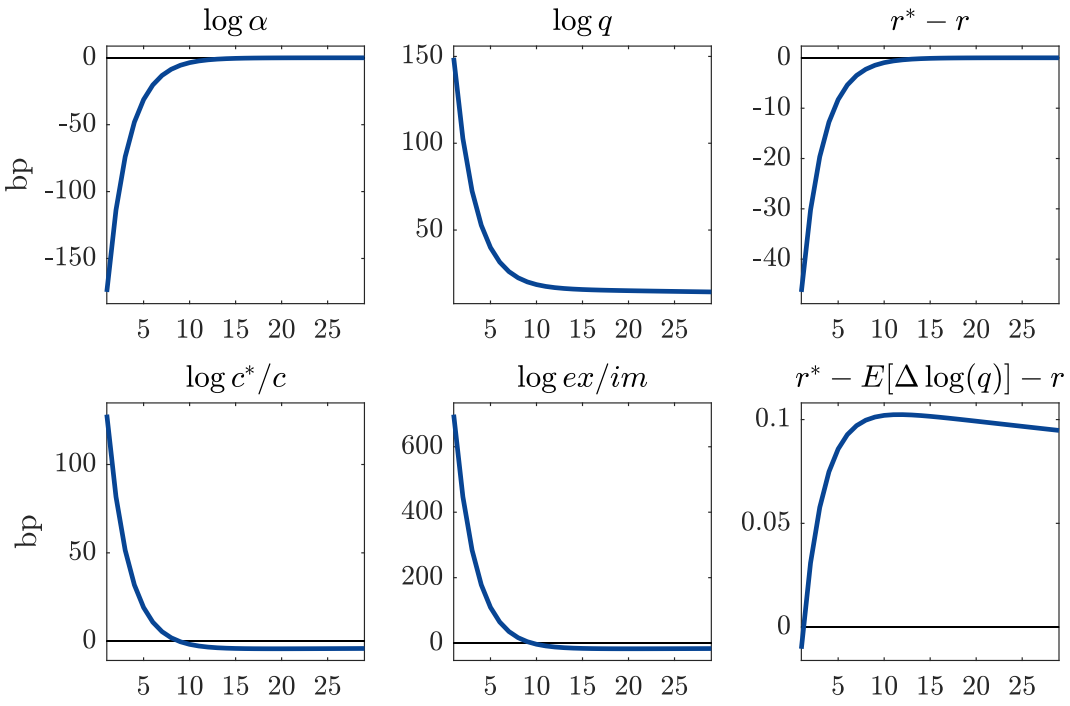

Figure 19: impulse responses to trade shock

appreciation is accompanied by a decline in U.S. net trade.[53] Relatedly, and also unlike demand and intermediation shocks, a dollar appreciation is accompanied by an increase in relative Foreign consumption, since Foreign borrows from the U.S. to finance its higher consumption of imports.[54] In terms of their effects on interest rates, trade shocks are like demand (or supply) shocks: a dollar appreciation is accompanied by an increase in U.S. interest rates versus Foreign interest rates.

Motivated by these effects, we discipline the stochastic properties of trade shocks to target the share of exchange rate variation explained by relative consumption at short horizons and unconditionally. As noted in Table 6 in the main text and Table 22 in this appendix, the R^2 values using relative consumption to explain the exchange rate are higher in the baseline model than in the data. As described in the fourth

[53] As described in footnote 36, the comovement induced by supply shocks depends on parameters.

[54] Since arbitrageurs are thus lending more to Foreign, the risk premium on Foreign bonds also rises, unlike demand shocks. In contemporaneous work, Bodenstein, Cuba-Borda, Goernemann, and Presno (2024) emphasize this effect of trade shocks and argue that it drives most exchange rate variation via endogenous UIP deviations. This channel is small in our calibration because the steady-state price of risk, Γ, is small. We note that while it can be amplified if Γ is higher, this would also imply that trade shocks, like γ_t shocks, induce an unconditional comovement between yield differentials and the exchange rate that is at odds with the data.

	Description	Value	Moment	Target	Model
β	U.S. disc. fact.	0.99758	$r^{(1)}$	0.97%	0.97%
β^*	Foreign disc. fact.	0.99708	$r^{(40)*} - r^{(40)}$	0.20%	0.20%
$\sigma^\beta, \sigma^{\beta^*}$	s.d. β, β^* shocks	0.0019	$\sigma(r^{(40)*} - r^{(40)})$	0.81%	0.80%
$\rho^\beta, \rho^{\beta^*}$	persistence β, β^*	0.98	$\rho_{-1}(r^{(40)*} - r^{(40)})$	0.93	0.92
ρ^{β,β^*}	corr. β, β^* shocks	0.84	$\sigma(\Delta r^{(40)})$	0.53%	0.52%
σ^z, σ^{z^*}	s.d. z, z^* shocks	0.005	$\sigma(\log y^* - \log y)$	1.73%	1.76%
ρ^z, ρ^{z^*}	persistence z, z^*	0.95	$\rho_{-1}(\log y^* - \log y)$	0.91	0.91
ρ^{z,z^*}	corr. z, z^* shocks	0.10	$\sigma(\Delta \log y)$	0.49%	0.51%
σ^γ	s.d. γ shocks	11	$\sigma(\Delta \log q)$	3.91%	4.27%
ρ^γ	persistence γ	0.85	$\rho_{-1}(\log \gamma)$	0.80	0.82
σ^α	s.d. α shocks	0.02	$R^2(\log q, \log c^*/c)$	0.29	0.34
ρ^α	persistence α	0.65	$R^2(\Delta \log q, \Delta \log c^*/c)$	0.03	0.04
ξ	pricing to market	1.3	$\sigma(\log s)/\sigma(\log q)$	0.27	0.28
Γ	arb risk pricing	$6E-4$	$\sigma(\log ex/im)$	11.41%	14.84%
σ	trade elasticity	0.9	$\sigma(\log q)$	11.48%	10.43%
ς	home bias	0.8	$(ex + im)/y$	0.25	0.23
ζ^*	rel. population	1.35	$\zeta^* q^{-1} y^*/y$	1.35	1.34

Table 26: calibrated parameters with trade shocks

Notes: data moments are estimated over 1991 Q2 – 2020 Q1. Model moments are averages over 1,000 simulations of 116 quarters each using a 1,000 quarter burn-in period. Externally set parameters in model are $\psi = 1$, $z = 1$, $z^* = 1$, and $\theta = 4$, the latter three all normalizations.

panel of Table 26, we use the volatility σ^α and persistence ρ^α of trade shocks to target these R^2 values for regressions in one-quarter changes and in levels. We reduce the volatilities of demand shocks $\sigma^\beta, \sigma^{\beta^*}$ so that the volatility of the exchange rate is no different than in the baseline model. To facilitate the comparison between this calibration and the baseline model, we leave all other parameters unchanged.

The resulting exchange rate comovements are more consistent with the data. Table 27 presents the analog to Table 22 but now with trade shocks added to the model. The signs of the comovements are all unchanged from the baseline model. But now, in the bottom two panels, the share of variation in the exchange rate explained by relative consumption or U.S. net trade is much lower than in the baseline model. At the same time, in the first two panels, the share of variation explained by yield

	1-qtr changes		4-qtr changes		12-qtr changes	
	Data	Model	Data	Model	Data	Model
$\log q$ on $r^{(1)*} - r^{(1)}$						
Coeff	[-4.54,0.19]	-0.62	[-4.03,1.22]	-0.64	[-2.75,1.46]	-0.76
Adj R^2	0.05	0.10	0.03	0.08	-0.00	0.09
$\log q$ on $r^{(40)*} - r^{(40)}$						
Coeff	[-6.42,0.87]	-7.59	[-6.52,-1.89]	-7.93	[-9.28,-2.46]	-8.68
Adj R^2	0.04	0.26	0.07	0.30	0.13	0.38
$\log q$ on $\log c^* - \log c$						
Coeff	[-2.70,-0.80]	-0.43	[-4.23,-1.80]	-0.77	[-6.25,-1.58]	-1.19
Adj R^2	0.03	0.04	0.13	0.11	0.27	0.23
$\log q$ on $\log ex/im$						
Coeff	[-0.33,0.17]	-0.06	[-0.51,0.30]	-0.15	[-0.75,0.24]	-0.30
Adj R^2	-0.01	0.02	-0.01	0.09	0.02	0.24

Table 27: exchange rate comovements in changes in data and model with trade shocks

Notes: model moments are averages over 1,000 simulations of 116 quarters each using a 1,000 quarter burn-in period.

differentials is not too much higher.

This model extension with trade shocks does not change our conclusion that relative demand shocks account for most of the variation in the exchange rate. Table 28 summarizes the share of variance in the exchange rate in levels and quarterly changes accounted for by each set of shocks. Mechanically, these shares are lower for demand shocks than in the baseline calibration because the volatility of these shocks was reduced to target the same exchange rate volatility. But it remains the case that, with trade shocks disciplined to match the explanatory power of relative consumption for the exchange rate, demand shocks account for most of the variation in the exchange rate. Figures 20 and 21 further make this point when we recover the path of $\{\epsilon_t^\alpha\}$ shocks to match the exact path of U.S. net trade over the 1991-2020 period (we continue to use 10-year yield differentials, output per capita, and the excess bond premium to recover the path of the other shocks). By construction, the model fit in Figure 20 is much tighter than in Figure 17 earlier in this appendix. But the resulting exchange rate path in Figure 21 is quite comparable to the baseline path in Figure 5,

	$\{\epsilon_t^{\beta}, \epsilon_t^{\beta^*}\}$	$\{\epsilon_t^{z}, \epsilon_t^{z^*}\}$	$\{\epsilon_t^{\gamma}\}$	$\{\epsilon_t^{\alpha}\}$
$\log q$	73%	3%	21%	3%
$\Delta \log q$	39%	3%	44%	14%

Table 28: variance decomposition in model with trade shocks

Notes: table reports shares of $\sigma^2(\log q)$ (first row) and $\sigma^2(\Delta \log q)$ (second row) due to each set of driving forces alone. Variances are averaged over 1,000 simulations of 116 quarters each using a 1,000 quarter burn-in period.

and indeed eliminating $\{\epsilon_t^{\alpha}\}$ shocks from the former does not much change it.

D.8 Present value decompositions

In the main text we explained that small-sample bias can explain why present value decompositions, as in Froot and Ramadorai (2005), suggest that expected interest rate differentials account for little of the variance in the exchange rate. Here we expand on this point.

Consider the standard identity

$$\begin{aligned} \log q_t &= \sum_{\tau=0}^{\infty} \mathbb{E}_t \left(r_{t+\tau} - r^*_{t+\tau} \right) + \sum_{\tau=0}^{\infty} \mathbb{E}_t \left(r^*_{t+\tau} - \Delta \log q_{t+\tau+1} - r_{t+\tau} \right) + \lim_{h \to \infty} \mathbb{E}_t \log q_{t+h}, \\ &\equiv \delta_t^{ir} + \delta_t^{rp} + \delta^q, \end{aligned} \tag{28}$$

where we assume the long-run value of the exchange rate (the last term) is finite and does not depend on t because the real exchange rate is stationary. It follows that the variance of the real exchange rate can be decomposed into the variance of expected interest rate differentials, variance of expected currency risk premia, and their covariance:

$$Var\left(\log q_t\right) = Var\left(\delta_t^{ir}\right) + Var\left(\delta_t^{rp}\right) + 2Cov\left(\delta_t^{ir}, \delta_t^{rp}\right). \tag{29}$$

In the data, it appears that expected risk premia account for most of the variance in the exchange rate. We use a VAR to construct the conditional expectations required to implement decomposition (29). We focus on a two-lag VAR in the log real exchange rate, three- and 10-year nominal yield differentials, and excess bond premium. As in the rest of the paper, we use the three-month nominal yield differential as a measure

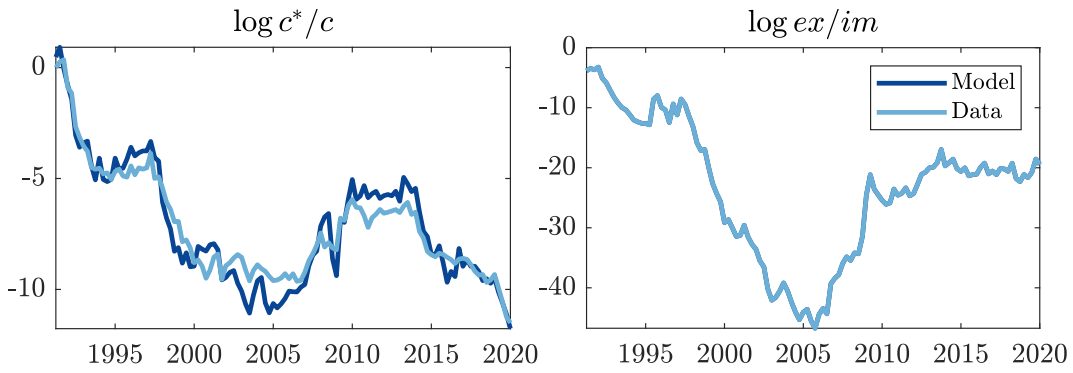

Figure 20: relative consumption and net trade in data and model with trade shocks

Notes: model-implied exchange rate simulated by inverting $\{\beta_t, \beta_t^*, z_t, z_t^*, \gamma_t, \alpha_t\}$ to match 10-year yields and output per capita in U.S. and G10, excess bond premium of Gilchrist and Zakrajsek (2012), and log U.S. net trade. All series plotted in *pp*. Constant is added to model-generated series to match same average value as data series.

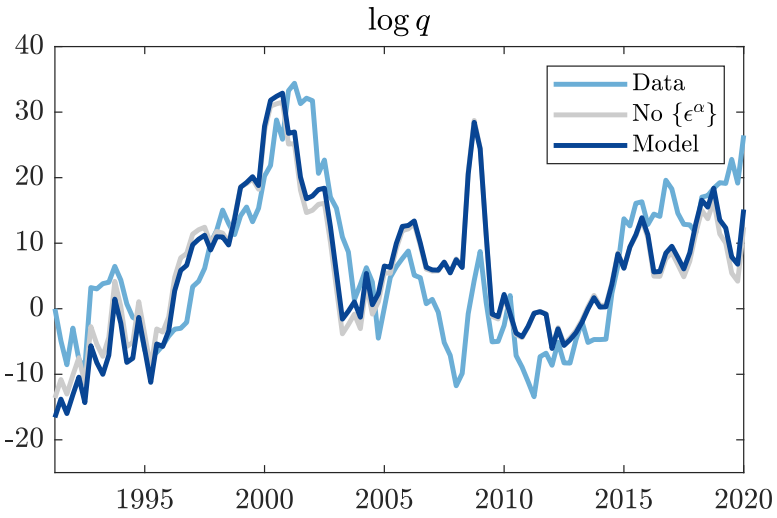

Figure 21: dollar/G10 exchange rate in data and model with trade shocks

Notes: model-implied exchange rate simulated by inverting $\{\beta_t, \beta_t^*, z_t, z_t^*, \gamma_t, \alpha_t\}$ to match 10-year yields and output per capita in U.S. and G10, excess bond premium of Gilchrist and Zakrajsek (2012), and log U.S. net trade. All series plotted in *pp*. Constant is added to model-generated series to match same average value as data series.

	Data	Model	Model	Model	Only $\{\epsilon_t^{\beta}, \epsilon_t^{\beta^*}\}$	Only $\{\epsilon_t^{\gamma}\}$
Sample	91Q2-20Q1	91Q2-20Q1	116 quarters*	116 quarters	116 quarters	116 quarters
VAR	yes	yes	yes	no	no	no
% $Var\left(\delta_t^{ir}\right)$	11 [2,47]	33	50	193	246	8
% $Var\left(\delta_t^{rp}\right)$	110 [73,186]	125	98	94	65	165
% $2Cov\left(\delta_t^{ir}, \delta_t^{rp}\right)$	-21 [-119,15]	-58	-39	-187	-211	-74

Table 29: decomposing variance of real exchange rate

Notes: each cell reports percentage points of $Var\left(\log q_t\right)$. In data, VAR to compute conditional expectations include 2 lags in log real exchange rate, 3m yield differential, 10y yield differential, and excess bond premium, and 90% confidence intervals using nonparametric bootstrap reported in brackets. In model, analogous VAR uses 2 lags in $\log q_t$, $r_t^{(1)*} - r_t^{(1)}$, $r_t^{(40)*} - r_t^{(40)}$, and $\log \gamma_t$. Second column uses shocks recovered from 1991-2020, and remaining columns are averages over 1,000 simulations of 116 quarters each using a 1,000 quarter burn-in period.
* This column reports medians instead of means because of large outliers in statistics implied by VAR in samples of only 116 quarters each.

of the expected real interest rate differential.[55] The first column of Table 29 reports that 110% of the variance in the dollar/G10 exchange rate over our maintained sample period is due to the variance in expected risk premia.

Our model reproduces the result that most of the variation in the exchange rate appears due to expected risk premia. In the second column of Table 29, we estimate a VAR on the data generated by the model using shocks recovered from 1991-2020 in the prior subsection. As in the data, the VAR features two lags and includes $\log q_t$, $r_t^{(1)*} - r_t^{(1)}$, $r_t^{(40)^*} - r_t^{(40)}$, and $\log \gamma_t$. The VAR run on the model implies that 125% of the variance in the exchange rate over this period is due to the variance in expected risk premia, comparable to the data. The third column of Table 29 averages the results from decompositions applied to many model-generated simulations of 116 quarters each, similarly finding that most of the variation in the exchange rate is due

[55]We obtain very similar results constructing expected real interest rates using nominal yields and expected inflation differentials. We also obtain similar results in specifications dropping the 10-year yield differential and excess bond premium, or adding more lags to the VAR.

to expected risk premia. This underscores that, from the perspective of the model, the shocks recovered over the 1991-2020 period are not unusual.

The reason for the dominant role of risk premia is that the VAR underestimates the persistence of interest rate differentials in small samples.[56] The fourth column of Table 29 uses actual, model-consistent expectations rather than those by implied by the VAR. We see that now, interest rate differentials account for most of the variance in the exchange rate.[57] The last two columns perform this decomposition given only demand or intermediation shocks (recalling that supply shocks contribute to little of the variance in the exchange rate). We see that the dominant role of interest rate differentials is driven by demand shocks. That said, our model does not imply that risk premium fluctuations are irrelevant: both due to intermediation shocks, and through the changes in arbitrageurs' exposure to exchange rate risk induced by demand shocks, time-varying currency risk premia also affect the exchange rate.

D.9 Comparison to Itskhoki and Mukhin (2021)

We next compare our results to those in Itskhoki and Mukhin (2021), on which we build. That paper concludes that currency intermediation shocks drive nearly all the volatility in the exchange rate. Here we describe why we reach a different conclusion.

There are two key differences between our calibration and that in Itskhoki and Mukhin (2021). First, the model in Itskhoki and Mukhin (2021) does not include demand (discount factor) shocks. Second and relatedly, intermediation shocks are calibrated differently than in our model. In particular, in Itskhoki and Mukhin (2021), intermediation shocks have quarterly autocorrelation of 0.97 (higher than our 0.85), and the volatility of intermediation shocks is calibrated to target a correlation between changes in the real exchange rate and relative consumption growth of -0.4.

Because of these differences, the calibration in Itskhoki and Mukhin (2021) features a larger role for intermediation shocks in driving exchange rate variation. In the absence of demand shocks, intermediation shocks are the only ones which can deliver a negative correlation between the exchange rate and consumption growth,

[56] This generalizes the standard result that there is downward bias in estimating the autocorrelation of a persistent process in small samples. See, for instance, Kendall (1954).

[57] It is small sample bias which explains these results, rather than any other misspecification in the VAR, because if we hypothetically had a much larger sample of data, we have verified that the VAR and model-consistent expectations would imply very similar variance decompositions.

consistent with our Proposition 1. The calibration thus features more volatile and, by assumption, persistent intermediation shocks.

Because intermediation shocks play a more important role, the model in Itskhoki and Mukhin (2021) implies a counterfactual comovement between the exchange rate and yield differentials. Table 30 reports key moments of interest regarding the exchange rate. The first three columns compare moments from the data, our model, and Itskhoki and Mukhin (2021). Both models generate comparable moments to the data in regards to exchange rate volatility, autocorrelation, predictability (or lack thereof), and comovement with relative consumption. However, the model in Itskhoki and Mukhin (2021) counterfactually implies that the dollar is strong when U.S. yields are relatively low in the last two rows. Figure 4 in the main text makes evident that this difference between models is clear even accounting for sampling uncertainty. The fourth column of Table 30 reports moments from our model without demand shocks, dropping the excess bond premium as a proxy for intermediation shocks, and instead disciplining the latter to target the volatility and persistence of the exchange rate directly.[58] The resulting moments are closer to those in Itskhoki and Mukhin (2021), including the comovement of the exchange rate with yield differentials. This clarifies that it is primarily the shocks included in the model and their calibration, rather than any other differences between models (such as endogenous production and nominal rigidities in Itskhoki and Mukhin (2021)), which account for the differences.[59] To visualize the implications of the counterfactual comovement with yield differentials, Figure 22 depicts the implied time-series of the 10-year yield differential when we recover intermediation shocks to match the observed exchange rate from 1991-2020. The implied 10-year yield differential is nearly the reverse of that in the data.

By adding demand shocks to the model and disciplining them using observed yield differentials, we are able to preserve the successes of Itskhoki and Mukhin (2021) while also matching the comovement between the exchange rate and yield differentials in the data. The last column of Table 30 reports moments in our baseline calibration with only demand shocks. Demand shocks disciplined by observed yield differentials already deliver a quite volatile exchange rate and negative correlation between the

[58]The calibration is detailed in Table 31.

[59]Relatedly, the working paper version of Itskhoki and Mukhin (2021) adds an additional shock which affects the exchange rate (expenditure share shocks) and the comovement between the exchange rate and short-term yield differential is flipped (see Table A2 in Itskhoki and Mukhin (2017)). The comovement with longer-term yield differentials is not reported.

	Data	Model	IM (21)	$\sigma^{\beta}, \sigma^{\beta^*} = 0$, γ targets q	Only $\{\epsilon_t^{\beta}, \epsilon_t^{\beta^*}\}$
Volatility and autocorrelation of real exchange rate					
$\sigma(\Delta \log q_t)/\sigma(\Delta \log c_t)$	7.82	4.95	5.67	4.97	6.15
$\rho(\log q_t)$	0.94	0.91	0.91	0.92	0.94
Exchange rate predictability					
$\Delta \log q_{t+1}$ on $r_t^* - r_t$	-0.74	-0.29	-2.73	-4.04	2.14
R^2 of $\Delta \log q_{t+1}$ on $r_t^* - r_t$	-0.00	-0.00	0.02	0.03	0.03
Exchange rate comovements					
$\rho(\Delta \log q_t, \Delta (\log c_t^* - \log c_t))$	-0.20	-0.77	-0.39	-0.76	-1.00
$\log q_t$ on $r_t^{(1)*} - r_t^{(1)}$	-3.28	-2.59	3.94	10.06	-7.36
$\log q_t$ on $r_t^{(40)*} - r_t^{(40)}$	-8.48	-9.40	31.20	23.62	-11.06

Table 30: moments in data, our model, and Itskhoki and Mukhin (2021)

Notes: model moments are averages over 1,000 simulations of 116 quarters each using a 1,000 quarter burn-in period. Column entitled "IM (21)" reports moments from Itskhoki and Mukhin (2021) obtained using online replication package and simulating calibration "IRBC+" (column 7 of Table 1 in that paper) in same way. In predictability regression, we regress change in nominal exchange rate on nominal interest rate differential, as we do in data. We price long bonds using the expectations hypothesis and we use nominal yield differential for $r_t^{(\tau)} - r_t^{(\tau)*}$, as we do in data. Column entitled "$\sigma^{\beta}, \sigma^{\beta^*} = 0$, γ targets q" reports results from calibration summarized in Table 31.

exchange rate and relative consumption. In this sense, observed yield differentials leave little room for intermediation shocks to account for much more exchange rate volatility, whether they have small volatility and high persistence, or larger volatility and lower persistence. We choose to discipline intermediation shocks with lower persistence than Itskhoki and Mukhin (2021) only because plausible proxies for these shocks from financial markets, such as the excess bond premium, imply low persistence. When these shocks have low persistence, they can account for deviations from UIP at high frequencies which a model with only demand shocks would miss.

D.10 Alternative calibrations

We finally detail the robustness of our results to alternative calibrations summarized in the main text.

Table 32 reports calibrated parameters when we allow relative demand, relative

	Description	Value	Moment	Target	Model
β	U.S. disc. fact.	0.99758	$r^{(1)}$	0.97%	0.97%
β^*	Foreign disc. fact.	0.99708	$r^{(40)*} - r^{(40)}$	0.20%	0.20%
σ^z, σ^{z^*}	s.d. z, z^* shocks	0.005	$\sigma(\log y^* - \log y)$	1.73%	1.74%
ρ^z, ρ^{z^*}	persistence z, z^*	0.95	$\rho_{-1}(\log y^* - \log y)$	0.91	0.91
ρ^{z,z^*}	corr. z, z^* shocks	0.10	$\sigma(\Delta \log y)$	0.49%	0.50%
σ^γ	s.d. γ shocks	6	$\sigma(\Delta \log q)$	3.91%	3.96%
ρ^γ	persistence γ	0.98	$\rho_{-1}(\log q)$	0.94	0.92
ξ	pricing to market	1.3	$\sigma(\log s)/\sigma(\log q)$	0.27	0.27
Γ	arb risk pricing	$2E-2$	$\sigma(\log ex/im)$	11.41%	12.02%
σ	trade elasticity	0.9	$\sigma(\log q)$	11.48%	10.59%
ς	home bias	0.8	$(ex+im)/y$	0.25	0.23
ζ^*	rel. population	1.35	$\zeta^* q^{-1} y^*/y$	1.35	1.35

Table 31: calibrated parameters given $\sigma^\beta = \sigma^{\beta^*} = 0$ and γ targeting q

Notes: data moments are estimated over 1991 Q2 – 2020 Q1. Model moments are averages over 1,000 simulations of 116 quarters each using a 1,000 quarter burn-in period. Externally set parameters in model are $\psi = 1$, $z = 1$, $z^* = 1$, and $\theta = 4$, the latter three all normalizations.

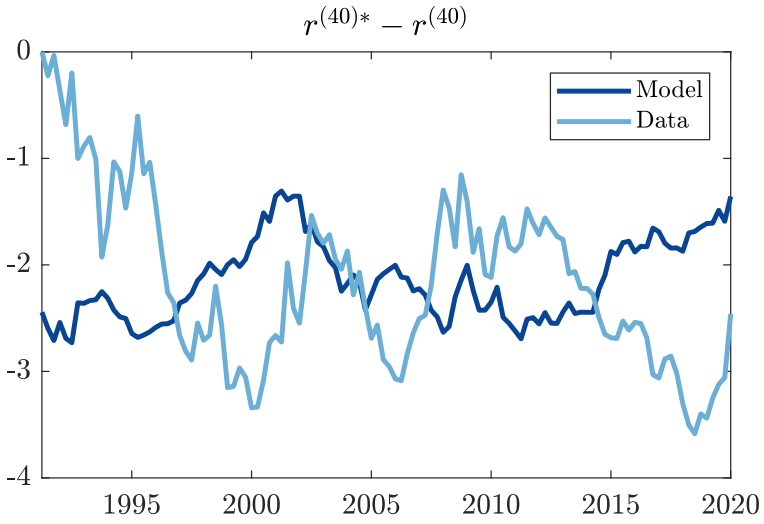

Figure 22: yield differential in calibration with $\sigma^\beta = \sigma^{\beta^*} = 0$ and γ targeting q

Notes: model-implied yield differential simulated by inverting $\{z_t, z_t^*, \gamma_t\}$ to match output per capita in U.S. and G10 and real exchange rate. All series plotted in *pp*. All yields are annualized.

supply, and intermediation shocks to be correlated with one another. These correlations are disciplined by the correlations between the 10-year bond yield differential, output per capita, and the excess bond premium. Table 33 demonstrates that even in this calibration we find that the demand wedges account for most of the variance in the exchange rate: the implied correlations between these wedges are not large enough to change our results.

Table 34 reports calibrated parameters when we target stochastic properties of the three-month rather than 10-year yield differential.[60] Since the three-month yield differential is even more persistent than the 10-year yield differential, this calibration implies an even more persistent process for relative demand than our baseline model. At the same time, the calibration implies slightly less volatile demand shocks than our baseline model, so that the ultimate variance decomposition of the exchange rate, reported in Table 35, remains quite comparable to our baseline. We find our baseline calibration more plausible since exchange rates depend on the expected future path of interest rates and long yields may better reflect this information than shorter-dated yields, given the interest rate smoothing of central banks.

[60]To facilitate comparison with the baseline calibration, we maintain the same average gap between β_t and β_t^*, disciplined by the average 10-year yield differential.

	Description	Value	Moment	Target	Model
β	U.S. disc. fact.	0.99758	$r^{(1)}$	0.97%	0.97%
β^*	Foreign disc. fact.	0.99708	$r^{(40)*} - r^{(40)}$	0.20%	0.20%
$\sigma^\beta, \sigma^{\beta^*}$	s.d. β, β^* shocks	0.002	$\sigma(r^{(40)*} - r^{(40)})$	0.81%	0.74%
$\rho^\beta, \rho^{\beta^*}$	persistence β, β^*	0.98	$\rho_{-1}(r^{(40)*} - r^{(40)})$	0.93	0.94
ρ^{β,β^*}	corr. β, β^* shocks	0.85	$\sigma(\Delta r^{(40)})$	0.53%	0.53%
σ^z, σ^{z^*}	s.d. z, z^* shocks	0.005	$\sigma(\log y^* - \log y)$	1.73%	1.71%
ρ^z, ρ^{z^*}	persistence z, z^*	0.95	$\rho_{-1}(\log y^* - \log y)$	0.91	0.92
ρ^{z,z^*}	corr. z, z^* shocks	0.20	$\sigma(\Delta \log y)$	0.49%	0.48%
σ^γ	s.d. γ shocks	11.5	$\sigma(\Delta \log q)$	3.91%	3.92%
ρ^γ	persistence γ	0.85	$\rho_{-1}(\log \gamma)$	0.80	0.82
$\rho^{\beta,z}$	corr. β and z	-0.30	$\rho(\Delta r^{(40)}, \Delta \log y)$	0.23	0.25
$\rho^{\beta^*,z}$	corr. β^* and z	-0.25	$\rho(\Delta r^{(40)*}, \Delta \log y)$	0.16	0.17
ρ^{β,z^*}	corr. β and z^*	-0.35	$\rho(\Delta r^{(40)}, \Delta \log y^*)$	0.42	0.36
ρ^{β^*,z^*}	corr. β^* and z^*	-0.45	$\rho(\Delta r^{(40)*}, \Delta \log y^*)$	0.38	0.40
$\rho^{\beta,\gamma}$	corr. β and γ	0.40	$\rho(\Delta r^{(40)}, \Delta \log \gamma)$	-0.52	-0.45
$\rho^{\beta^*,\gamma}$	corr. β^* and γ	0.40	$\rho(\Delta r^{(40)*}, \Delta \log \gamma)$	-0.35	-0.32
$\rho^{z,\gamma}$	corr. z and γ	-0.45	$\rho(\Delta \log y, \Delta \log \gamma)$	-0.25	-0.28
$\rho^{z^*,\gamma}$	corr. z^* and γ	-0.20	$\rho(\Delta \log y^*, \Delta \log \gamma)$	-0.33	-0.32
ξ	pricing to market	1.3	$\sigma(\log s)/\sigma(\log q)$	0.27	0.27
Γ	arb risk pricing	$6E-4$	$\sigma(\log ex/im)$	11.41%	11.61%
σ	trade elasticity	0.9	$\sigma(\log q)$	11.48%	10.01%
ς	home bias	0.8	$(ex + im)/y$	0.25	0.23
ζ^*	rel. population	1.35	$\zeta^* q^{-1} y^*/y$	1.35	1.34

Table 32: calibrated parameters with fully correlated shocks

Notes: data moments are estimated over 1991 Q2 – 2020 Q1. Model moments are averages over 1,000 simulations of 116 quarters each using a 1,000 quarter burn-in period. Externally set parameters in model are $\psi = 1$, $z = 1$, $z^* = 1$, and $\theta = 4$, the latter three all normalizations.

	$\{\epsilon_t^{\beta}, \epsilon_t^{\beta^*}\}$	$\{\epsilon_t^{z}, \epsilon_t^{z^*}\}$	$\{\epsilon_t^{\gamma}\}$
$\log q$	78%	3%	25%
$\Delta \log q$	46%	3%	57%

Table 33: variance decomposition in calibration with fully correlated shocks

Notes: table reports shares of $\sigma^2(\log q)$ (first row) and $\sigma^2(\Delta \log q)$ (second row) due to each set of driving forces alone. Columns do not sum to 100% because shocks are correlated. Variances are averaged over 1,000 simulations of 116 quarters each using a 1,000 quarter burn-in period.

	Description	Value	Moment	Target	Model
β	U.S. disc. fact.	0.99758	$r^{(1)}$	0.97%	0.97%
β^*	Foreign disc. fact.	0.99708	$r^{(40)*} - r^{(40)}$	0.20%	0.20%
$\sigma^{\beta}, \sigma^{\beta^*}$	s.d. β, β^* shocks	0.0012	$\sigma(r^{(1)*} - r^{(1)})$	1.58%	1.62%
$\rho^{\beta}, \rho^{\beta^*}$	persistence β, β^*	0.99	$\rho_{-1}(r^{(1)*} - r^{(1)})$	0.96	0.90
ρ^{β,β^*}	corr. β, β^* shocks	0.60	$\sigma(\Delta r^{(1)})$	0.51%	0.56%
σ^{z}, σ^{z^*}	s.d. z, z^* shocks	0.005	$\sigma(\log y^* - \log y)$	1.73%	1.74%
ρ^{z}, ρ^{z^*}	persistence z, z^*	0.95	$\rho_{-1}(\log y^* - \log y)$	0.91	0.91
ρ^{z,z^*}	corr. z, z^* shocks	0.10	$\sigma(\Delta \log y)$	0.49%	0.51%
σ^{γ}	s.d. γ shocks	11.5	$\sigma(\Delta \log q)$	3.91%	3.89%
ρ^{γ}	persistence γ	0.85	$\rho_{-1}(\log \gamma)$	0.80	0.82
ξ	pricing to market	1.3	$\sigma(\log s)/\sigma(\log q)$	0.27	0.27
Γ	arb risk pricing	$5E-3$	$\sigma(\log ex/im)$	11.41%	11.63%
σ	trade elasticity	0.9	$\sigma(\log q)$	11.48%	10.22%
ς	home bias	0.8	$(ex + im)/y$	0.25	0.23
ζ^*	rel. population	1.35	$\zeta^* q^{-1} y^*/y$	1.35	1.35

Table 34: calibrated parameters using three-month yields

Notes: data moments are estimated over 1991 Q2 – 2020 Q1. Model moments are averages over 1,000 simulations of 116 quarters each using a 1,000 quarter burn-in period. Externally set parameters in model are $\psi = 1$, $z = 1$, $z^* = 1$, and $\theta = 4$, the latter three all normalizations.

	$\{\epsilon_t^{\beta}, \epsilon_t^{\beta^*}\}$	$\{\epsilon_t^{z}, \epsilon_t^{z^*}\}$	$\{\epsilon_t^{\gamma}\}$
$\log q$	77%	4%	20%
$\Delta \log q$	47%	4%	50%

Table 35: variance decomposition in calibration using three-month yields

Notes: table reports shares of $\sigma^2(\log q)$ (first row) and $\sigma^2(\Delta \log q)$ (second row) due to each set of driving forces alone. Variances are averaged over 1,000 simulations of 116 quarters each using a 1,000 quarter burn-in period.